Sea Breeze Cooling Power in the Adelaide Metropolitan Area

Submitted by Saeedeh Gharib Choobary

In Partial Fulfilment of the Requirements for the Degree of Master of Science by Research

School of the Environment

Faculty of Science and Engineering

Flinders University

May 2017

Contents

List of Figures

List of Tables

Summary

Coastal cities, such as Adelaide in South Australia located approximately 10 km to the east of St Vincent Gulf, benefit from sea breeze cooling in summer months. Although the kinematics and dynamics of sea breeze and its interaction with urban climate have been widely studied in the literature, quantitative analysing the cooling role of sea breeze has been unattended. The sea breeze occurrence and cooling effect during its inland progress to the Adelaide Central Business District (CBD) are investigated using high spatial and temporal resolution meteorological data during the summer months between 2010 and 2013. A new approach to quantify the sea breeze cooling effect of is presented by introducing a quantitative parameter, Sea Breeze Cooling Power (SBCP), with the unit of °C·min. The results indicate that a declining trend in the Cumulative Sea Breeze Cooling Power (CSBCP) during the sea breeze inland advance for all summer months at an average rate of -45.5 °C.min/km inland from the coastline, with an average effective penetration depth of 13.8 km. Moreover, December shows the highest CSBCP, followed by January, February and March, respectively. Also, in the Adelaide CBD the frequency of the sea breeze cooling at a 30-minute time interval is significantly higher in noon and early afternoon compared to the morning time for all the months. In addition, the average of daily maximum cooling due to the sea breeze passage (dT_{max}) in January, February and December is as significant as 1°C in the Adelaide CBD. The dT_{max} in CBD is reduced by almost 50 percent in March compared to other summer months.

Declaration

I certify that this thesis does not incorporate without acknowledgment any material previously submitted for a degree or diploma in any university; and that to the best of my knowledge and belief it does not contain any material previously published or written by another person except where due reference is made in the text.

Signed.....*Saeedeh Gharib Choobary*.....

Date.....11/May/2017.....

Acknowledgments

I would like to thank my principal supervisor Dr Huade Guan for his time, ideas, expertise, feedback, and encouragement. I would also like to thank my co-supervisor Dr Jochen Kaempf for his kind support during the thesis preparation.

I am thankful to the South Australia's Department of Premier and the Cabinet, and Department of Environment, Water and Natural Resources as this study was funded in part by the Department, through the University Sector Agreement Research Fund through a joint research project "City of Adelaide Urban Heat Island Micro-Climate Study" between Flinders University and the Adelaide City Council. The project is also supported by the Goyder Institute for Water Research. The Adelaide urban heat island monitoring network was funded by South Australia's Department of Planning and Local Government (then) and Flinders University. The network is maintained by Flinders University, with support from South Australia Power Network, Adelaide City Council, Bureau of Meteorology, and Environmental Protection Authority. I am grateful to the all supporters mentioned above.

The authors thank Dr John Bennett, Dr Caecilia Ewenz, Dr Vinod Kumar, Chris Kent and Chuanyu Zhu for their assistance with data collection.

And last but not least, I want to express my gratitude to my husband, Mehrdad for his full support during the journey, especially for his encouragement to move forward when I was really tired.

1. Introduction

Sea Breeze Development

The most iconic climate pattern of coastal areas is the sea breeze development and circulation over the area during the day which could be followed by night time land breeze as well. The temperature difference between the air over the hot land and over the cool water causes the sea breeze which flows inland during daytime. Also, the more rapidly temperature decline over the land comparing to the ocean over the night time, can drive an offshore wind called land breeze over night time (Gille et al., 2005). The temperature difference should be large enough to produce the sufficient pressure gradient for the sea breeze and land breeze to be established, especially when the direction and speed of the prevailing synoptic winds weakens these wind patterns (Simpson, 1994). According to the study mentioned study, the sea breeze arrival can be expected regularly every day, if the gradient of pressure stays stable over the coastal area such as tropical countries with hot weather. Sea breeze is also expected to be developed on sunny days in temperate coastal regions with a thickness depth of a few meters into the air above it early in the day up to hundreds of meters depth until the later times of the day (Simpson, 1994). As the day develops, the wind direction shifts due to the rotation of the earth and the sea breeze gradually advances inland and over the ocean as well (Miller et al., 2003).

The pressure field growth which causes the sea breeze flow can be affected by the complexity of the coast line as well as the presence of the significant features such as mountains near to the coast (Simpson, 1994).

In an ideal straight coastline with unvarying inland condition, sea breeze hodographs show an eclipse with clockwise wind rotation. However, coastal complexity and the anabatic winds from

the mountains located within 10 to 20 kilometres from coasts may change ideal direction of rotation to anticlockwise rotation (Simpson, 1994).The phenomenon was well studied by Kusuda & Alpert (1983) theoretically.

Kinematics and dynamics of sea breeze have been widely studied based on theories and observations. The subjects in the sea breeze literature were well summarized by Miller et al. (2003).

Although the occurrence and physical mechanisms of sea breeze has been well investigated, the influence of the phenomenon on local climate in urbanized areas is under-attended. The meteorology of coastal regions, pollutant dispersal and air quality of coastal cities can be highly influenced by the sea breeze wind pattern over the coastal area (Gille et al., 2005).

Effect of Sea Breeze on Air Pollution Transportation in Cities

Sea breeze in the coastal urbanized area also influences pollution transportation (e.g., Physick, 1976 ;Lalas et al., 1983; Lu et al., 1994; Clappier et al., 2000; Ding et al., 2004; Mavrokou et al., 2012; Loughner et al., 2014). For example the effect of sea breeze on the episodes of photochemical smog was analysed by using numerical modelling and field observations in the Greater Athens area on the three selected days of 12 to 14 of September 1994 (Clappier et al., 2000). The selected days were representative of the two common air flow patterns in the Athens peninsula summer time. The pollution level by each of the flow patterns is significantly different. The sea breeze inland advance was weaken by the strong northerly prevailing winds on 12th and 13th of September which led to the low ozone concentration over the Greater Athens in the two days. Besides, on 14th of September when the synoptic winds were weak, the sea breeze inland flow raised the ozone concentration over the east and north of the city.

The role of sea breeze on transportation of pollutants was also studied in Adelaide, the capital

city of South Australia during the summer months of 1972-1973 and 1973-1974 (Physick, 1976). The air over the shore line of the city which is located by the gulf of St Vincent showed colour change in summer mornings. The results of numerical modelling and filed measurements show that at night, the land breeze transports the trapped pollutants toward the gulf making the air over the water discoloured in the early morning. Then the pollution is recycling back to the city by the sea breeze of the next day.

Sea breeze coming from the sea surface has different air properties from the urban air, and thus may modify the weather in the area under the sea breeze influence. However, few studies have mentioned the effect of sea breeze on spatial and temporal distribution of temperature relief in urban areas, which are summarized in the following.

Sea Breeze Influence on Thermal Environment of Cities

In coastal urbanized areas, sea breeze interacts with urban heat island circulation (HIC), enhances urban frictional drag (e.g., Yoshikado et al., 1992; Cenedese et al., 2003; Freitas et al., 2007; Sashiyama et al., 2014). For example the effect of sea breezes obstruction by high-rise buildings on the night time urban heat island was analysed for an area near Tokyo bay in Minato City in the Tokyo Metropolis (Sashiyama et al., 2014). Geographic Information Systems (GIS) and a model for weather simulation were applied to compare the city thermal environment and wind flow in the presence and no-presence of the high-rise buildings. The results show that in the area located five to ten kilometre downwind of the high-rise buildings, temperature increased by approximately 3°k and a wind speed dropped by approximately 1 m/s between 6 p.m. and 9 p.m. Also, the sea breeze obstruction leads to the higher temperature in that area for that time period, which influences the formation of the urban heat island during the night.

Most published studies used qualitative approaches to study sea breeze effects on thermal and biometeorological environment of the coastal cities respectively. The quantitative analysis is commonly conducted based on temperature and thermal comfort indexes. In addition, the evaluations are mostly restricted to the days with typical meso scale meteorological conditions (e.g. typical heat wave days, clear sea breeze days, etc).

The inland penetration of sea breeze in New York City and its influence on the UHI centre displacement was examined by Gedzelman et al. (2002). It was found that in the days with afternoon sea breeze, the coastal area and New York City was cooled more than the inland area in summers 1997-98, causing the average of UHI with its smallest value over the day occurring in midnight followed by a displacement of 10 km in UHI towards the west of the city.

Masuda et al. (2005) carried out observations and wind tunnel experiments on a coastal skyscraper close to the Tokyo bay and an inland city station to evaluate the temperature and wind field distribution under the influence of sea breeze in the study area during two consecutive summer days. The observation showed the city station is 1.4 °C warmer than the coastal station on average, which was attributed to the effect of the urban structure on making the wind field weak and unstable.

The effect of sea breeze on the temperature distribution was also noted in a case study by Emmanuel and Johansson (2006) on the UHI of Colombo metropolitan area in Seri Lanka during a two-week monsoon period. The results revealed that the urban areas which were closer to the sea and had a larger height to width ratio experienced lower temperature during the study period.

An average temperature difference by 4°C between a river (Tangus) bank and an inland measurement point in the Lisbon city in Portugal during sea breeze days with weak synoptic

winds of the summer 2004 was reported by Alcoforado et al. (2009). In addition, the calculated Physiologically Equivalent Temperature (PET) was 3°C cooler in the near river areas compared to an inland station.

Papanastasiou et al. (2010) studied the influence of the sea breeze development on thermal comfort and pollution levels of a coastal urban site and an inland suburban location during the two heat wave days of 25th July and 26th Jun in 2007 on the east coast of central Greece. Analysing the meteorological data, the sea breeze day of 25th July showed significantly lower daytime temperature than the non-breeze day of 26th Jun in the study in the coastal urban site. The difference in daily temperature of the two studied days reached its maximum of 8°C towards the afternoon when the sea breeze strength was maximum in 25th July (Papanastasiou et al., 2010).

lopes et al. (2011), studied the variation of PET in the Funchal city in Madeira island to assess the thermal comfort distribution in the city during the selected sea breeze days of summer 2006 for tourism planning studies. It was investigated that in the coastal station the temperature was about 4°C to 5°C less than the urban stations on average in hot days in which the maximum temperature was more than 32°C and minimum temperature more than 24°C. Moreover, the temperature difference by 8°C in PET after the sea breeze onset was found in the coastal station in a selected hot day.

In the UHI study over the Bilbao city in the northern Spain by Acero et al. (2013), significant apparent UCI occurs after middays in summer and spring. It was found to be related to the more intense sea breeze penetration over the city compared to the rural areas in which the sea breeze is blocked by the mountainous topography. Moreover, the daytime temperature of the stations closer to the shoreline was found to be always cooler than the inland areas with higher

anomaly in the more frequent sea breeze seasons of spring and summer.

In addition, the sea breeze interaction with urban morphology has been studied and implemented in urban planning. For example, sea breeze has been included in urban planning in Tokyo, by applying new development plans using numerical modelling on the Earth simulator and wind tunnel experiments to increase ventilation paths from the coastal areas to the Tokyo city centre (Kagiya and Ashie 2009).

Moreover, a CFD numerical simulation in a large scale was applied to investigate the effect of the urban morphology on temperature distribution and local ventilation in the city of Tokyo for 31st of July 2005 considering the small scale vortices in urban space (Ashie et al., 2009). The results revealed that the areas on the both sides of Sumida River through which the sea breeze flows had lower temperatures compared to the inland areas and the breeze advances inland to almost 100-200 meters.

In addition, the effect of Tokyo city development from 1970s to 1990s on the city thermal field, was investigated by applying a meso scale meteorological simulation MM5 conducted by Kato and Hiyama (2012). The modelling was run for a day with clear sea breeze as the control simulation and the results were compared to the runs with modified urban surface parameters as the reflection of the urbanization process in Tokyo. The findings presented that urbanization has led to 0.77°C more elevated surface temperature in the selected inland station compared to the coastal station which had ventilation from the Tokyo bay breeze.

Significance of the Study

There are limited studies on sea breeze cooling effect in the metropolitan area in Adelaide, the capacity of South Australia. Guan et al. (2013) reported a coast-inland temperature gradient of 0.03^{o}C /km based on long term average monthly maximum temperature. A temperature

difference of almost 4°C between a reference coastal station and the hot spots in the Adelaide CBD was presented for the days with the maximum temperature over 35°C for summer months 2011-2013 (Guan et al., 2016).

According to Australian Bureau of statistics 2012-2013 an estimated population of 1.29 million people live in Adelaide, the fifth largest city of Australia. It has hot and dry summers and increasing heatwaves intensity and frequency (Sturman and Tapper 1996).

The adverse negative socio-economic and environmental impact of high temperature including energy demand increase, human health problems, water demand rise, tourism preference shift, emphasises the importance of applying new mitigation and adaptation strategies in the area. Although most of the adaptation procedures focus on urban design as well as anthropogenic heat control factors, the potential cooling role of natural resources such as sea breeze events in the prospect of a sustainable coastal city has been ignored. Thus the sea breeze cooling capability in hot summer of coastal cities, such as Adelaide, should be estimated and quantified.

Objectives of the Study

The objectives of this study are (1) to quantify the sea breeze cooling effect over the Adelaide metropolitan area, and (2) to examine how this effect varies in summer months and with the distance from the coast. A new quantitative parameter, Sea Breeze Cooling Power (SBCP) is introduced in this study to evaluate the pattern of cooling power strength during the cool air inland advance.

2. Study Area

Geographical location of the Adelaide Central Business. District

The study area is concentrated between the coast line and the Adelaide Central Business District (CBD), the metropolitan centre of the greater Adelaide (Fig.1a). The CBD with an estimated area of 10.5 km^2 is separated from the surrounding suburbs by a belt of parklands (Fig. 1).

Urban Climate Zone Classification of the Adelaide CBD

According to the Urban Climate Zone (UCZ) classification by (Oke, 2006), the built environment of the north-to-south to the centre of the CBD can be defined with the close set of high-rise apartments and office buildings (Fig. 1C). This is constituted of the UCZ of category one which reflects this portion of the city mostly business focused. The business centre is surrounded by the high density and medium density urban structure making up the residential portion of the city centre. Also the green area of the central square of the city, and the surrounding parklands are matched with UCZ 6 (Fig. 1d). Table 1 shows the related UCZ of the distributed temperature sensors in the Adelaide CBD, Adelaide Airport, Netley and Kent Town weather station.

Climate of Adelaide

Adelaide has a Mediterranean type climate with a wet and mild-to-cold winter as the result of northward movement of the low pressure belt on the southern ocean to the region which pushes the subtropical high pressure belt to the continent interior. According to the BOM (2017), the mean of annual rainfall in Kent Town weather station is 551 mm in years between 1978 and 2016 with Jun, July and August recorded as the wettest months in the mentioned years. On the other hand, summers are dry and warm-to-hot as the belt of subtropical high pressure system displaces well to the south of the continent.

According to the Bureau of Meteorology (BOM) (2015), a mean maximum temperature of 29.4°C, 29.4°C, 27.1°C was recorded at the Kent Town weather station for years 1977 to 2014 in January, February and December, respectively. About 6 days, 5 days and 3 days more than 35°C per month in average were recorded for the three summer months, respectively in the report. In the summer months of 2011-2013, it is reported that 57 days in the three years had the daily maximum temperature over 35 °C (Guan et al. 2016).

The climate of Adelaide is largely influenced by seasonal synoptic winds. In winter and autumn, the dominant wind directions are from north and north-east in the morning with no dominant wind direction detected for spring and summer mornings, however the observations show the arrival of south-westerly winds is more prevailing in the afternoon of summer months (Pazandeh, 2015). Also, in summer months, the Adelaide climate is largely affected by the winds generated locally such as the sea breezes and gully winds from the Mt Lofty, however the wind flows in winter is significantly controlled by the prevailing synoptic winds (Lyons, 1975).

Moreover, analysis on the spatial and temporal pattern of the thermal environment of the Adelaide CBD and its surrounding suburbs, presents an estimated night time UHI, defined as the elevated temperature in the Adelaide CBD compared to the surrounding parklands, of almost 2.5°C for the CBD in the summer months 2011-2013 (Guan et al. 2016). However, during the summer day time of the mentioned study over the Adelaide region, quantification of the UHI was difficult due to the interacting role of the sea breeze flow on the CBD thermal climate, but the sea breeze inland advance causes the west-east day time thermal gradient (Gharib & Guan, 2015). UHI, was also clearly observed in the Adelaide CBD based on various observational and mathematical modelling approaches since 2009 (Vinodkumar et al. 2012).

Therefore, the abnormal high temperature records besides the coastal location of the Adelaide city which is approximately 10 km to the eastern coast of St Vincent Gulf, emphasises the potential role of the summer sea breeze as a natural cooling resource on heat relief in the area.

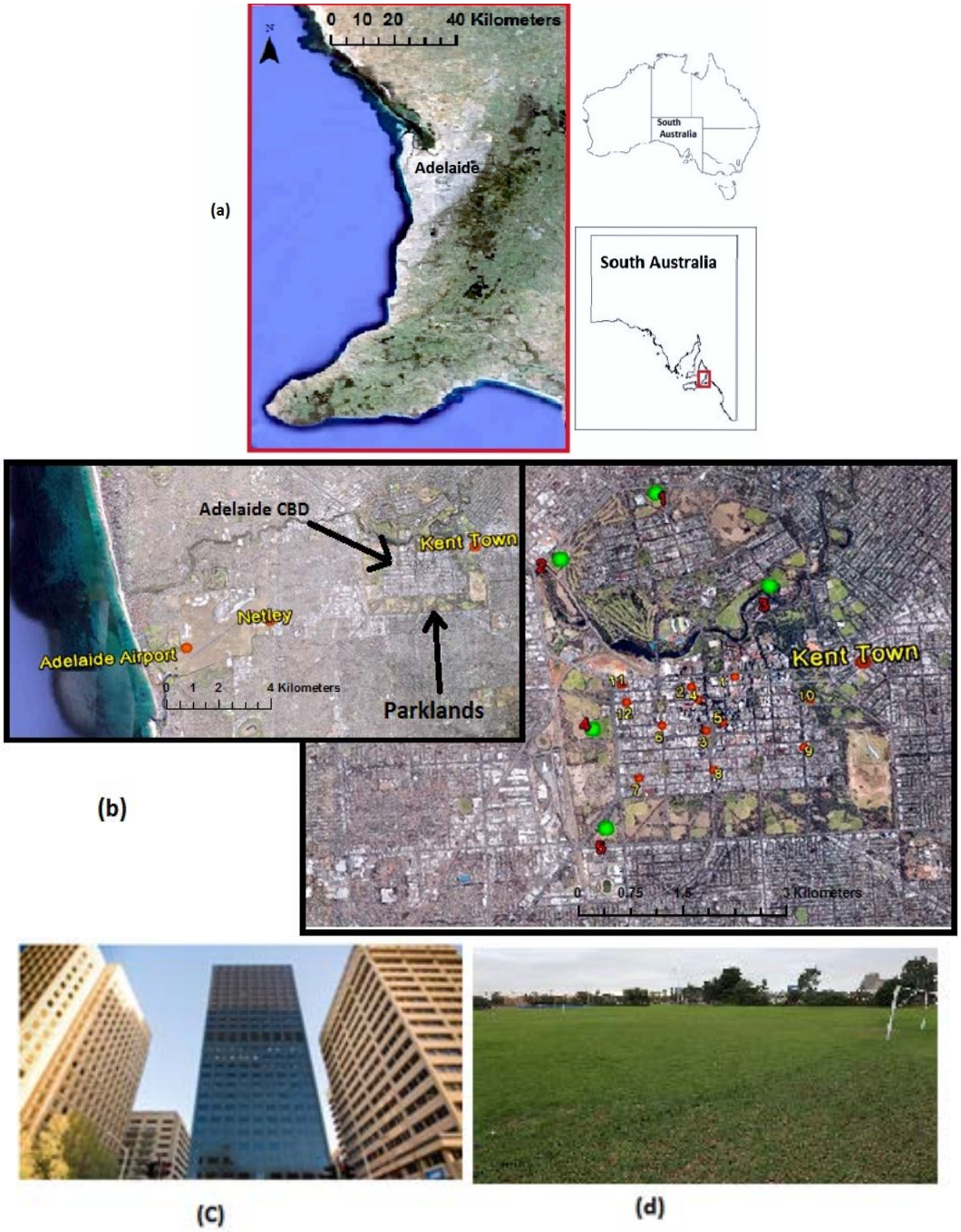

Figure 1: Study Area (a) Location of the capital city of south Australia, Adelaide, (b) (Left) Location of the Adelaide CBD and Parklands and of the Automatic Weather Stations (AWS), Adelaide Airport, Netley and Kent Town and (Right) Distribution of the Ibutton Thermochron sensors in the Adelaide CBD and Parklands, (c) Grenfell Street (UCZ 1), (d) Adelaide West Parklands (UCZ 6).

Table 1: Urban Climate Zone (UCZ) classification for the stations presented in Figure. 1

Station Number	Related Urban Climate Zone (UCZ)
1,2,4,5	UCZ 1
6,11,12	UCZ 2
7,8,9	UCZ 3
3,10	UCZ 6
Adelaide Airport	UCZ 5
Kent Town Weather Station	UCZ 6
Netley Weather Station	UCZ 5

3. Methodology

Field Measurements and Data Collection

The occurrence and cooling effect of the sea breeze onset during its inland advance to the Adelaide CBD is investigated using high spatial and temporal resolution of meteorological data during the summer months between 2010 and 2013. Although January, February and December are formally considered as the summer months for the study area, but considering the historical records of the abnormal high temperatures or even the heat waves in March, the month is also categorized as summer season in the present study. So, the total number of sample days of the study are 364 days which includes 12 summer months between 2010 and 2013, however the rainy and cloudy days are excluded from the analysis as will be described in more details later in this chapter and chapter 4.

Meteorological data including ambient air temperature, relative humidity, wind direction and wind speed in high temporal resolution gathered from automatic weather stations (AWS) installed in the Adelaide Airport and Kent Town, at 6m height (Fig.1b). The data was provided by the Bureau of Meteorology. Meteorological data collected at the Netley Automatic weather station installed by the Adelaide Environmental Protection Authority (EPA) is also included in the analysis. The instrument technical characteristics as well as their distance from the coast are summarized in Table 2 and Table 3, respectively. The coastal distance in Table 3 is the orthogonal distance of the stations from the coast line.

Table 2: Technical details of the Automatic Weather Stations (AWS) and Ibutton Thermochron sensors

Site name	Measured Parameter at Site	Logger Commercial Name	Sensor Commercial Name	Sensor Resolution	Sensor Accuracy	Data Recording Temporal resolution
Kent town	Wind Speed	Almos AWS	Synchrotac 732	0.5 m/s	±2.5 m/s	10
Kent town	Wind Direction	Almos AWS	Synchrotac 732	1.5°	±10°	10
Kent town	Dry bulb Temperature	Almos AWS	Rosemount ST2401	0.1°C	±0.4°C	10
Kent town	Wet Bulb Temperature	Almos AWS	Rosemount ST2401	0.1°C	±0.4°C	10
Kent town	Mean Sea Level Pressure	Almos AWS	Vaisala PTB330B	0.01hPa	±0.5hPa	10
Adelaide Airport	Wind Speed	Almos AWS	Synchrotac 732	0.5 m/s	±2.5 m/s	10
Adelaide Airport	Wind Direction	Almos AWS	Synchrotac 732	1.5°	±10°	10
Adelaide Airport	Dry bulb Temperature	Almos AWS	Rosemount ST2401	0.1°C	±0.4°C	10
Adelaide Airport	Wet Bulb Temperature	Almos AWS	Rosemount ST2401	0.1°C	±0.4°C	10
Adelaide Airport	Mean Sea Level Pressure	Almos AWS	Vaisala PTB330B	0.01hPa	±0.5hPa	10
Netley	Wind Speed	Vaisala QML201C	WS425 ultrasonic wind sensor	0.1 m/s	±0.135m/s	10
Netley	Wind Direction	Vaisala QML201C	WS425 ultrasonic wind sensor	1°	±0.2°	10
Netley	Temperature	Vaisala QML201C	HMP45D Temperature Sensor	0.1°C	±0.2°C	10
Netley	Mean Sea Level Pressure	Vaisala QML201C	PMT16A pressure sensor	0. 1hPa	< ± 0.3 hPA	10
CBD stations	Temperature	Thermochron Ibutton DS1922L-F5	Thermochron Ibutton DS1922L-F5	0.0625 °C	±0.5°C	30
Parkland Stations	Temperature	Thermochron Ibutton DS1922L-F5	Thermochron Ibutton DS1922L-F5	0.0625 °C	±0.5°C	30

Table 3: Geographical Information of Data Collection Sites

Site Name	Elevation Above Sea Level(m)*	Coastal Distance(km)
Kent Town	48	10.8
Adelaide Airport	8.2	1.1
Netley	29	3.9
CBD Stations	48	8.8
Parkland Stations	39	8.8

* The elevation above mean sea level for CBD and Parkland sensors are the average of all the installed sensors in the locations

Spatial and temporal variations of the ambient air temperature over the Adelaide CBD and the parkland belt were analysed using the data from the Urban Heat Island Project conducted by the Flinders University of South Australia. In order to represent the urban climate of the CBD, the Maxim Integrated Products Thermochron Ibuttons temperature loggers with a temperature resolution of ±0.0625°C used in the project, were installed in city locations with various built environment characteristics. Guan et al. (2013) reports a good agreement between the measured temperatures by the ibutton sensors in the shields and the measurements of the ambient temperature by the Bureau of Meteorology in a standard Stevenson screen.

A precision quartz crystal thermometer was used to calibrate the sensors to yield temperature (Guan et al., 2013). The calibrated accuracy was to be higher than 0.12°C.

The network of instrumentation provided data for 12 stations in the CBD and the surrounding parklands. The sensors were installed in locations with free air flow and away from buildings walls to avoid the idiosyncratically local effects on measurements. The sensors are protected from rain by louvered radiation shields. The shields also minimize the effects of thermal and

solar radiation on the sensors measurements. In addition, the material of the shields which are thermally insulating and the white painting of the shields which backscatters the incident solar radiation, help to reduce the effect of daily solar radiation as well as night time cooling due to radiation of thermal emission. The loggers adjusted to record the ambient air temperature at 4 meter height above the ground with a temporal resolution of 30 minutes. The distribution of the sensors over the Adelaide CBD and the parklands is shown in Fig.1b. Fig.2.a shows a group of the Ibutton sensors installed on a board for calibration. Also an example of a temperature measuring site in the Adelaide CBD is presented in Fig.2.b. The logger technical characteristics is also summarized in Table 2.

(a)

(b)

Figure 2: (a) A collection of Maxim Thermochron Ibutton sensors set up for calibration, (b) An ibutton placed in the louvred radiation shield and mounted from a lighting standard pole in the CBD (Guan et al., 2013).

Detection of Sea Breeze Onset in the Study Area

The inland advance of sea breeze accomplishes with a variety of meteorological signs which has been the subject of observational and theoretical studies. For example, the structure of the sea breeze leading edge and its interaction with the ambient air as well as the effect of the synoptic weather on the frontal advance was studied by Wakimoto and Atkins (1994), Hadi et al. (2002), Suresh (2007) and Muppa et al. (2012) using radar measurements at boundary layer and satellite images.

In addition, field measurements including data of ambient air temperature and wind flow parameters has been the core of a wide range of data analysis to determine sea breeze circulation characteristics (e.g. Frizzola and Fisher, 1963, Johnson and O'brien, 1973, Clappier et al., 2000, Bastin et al., 2005, Lin et al., 2008, Arrillaga et al., 2016).

Moreover, analytical and numerical modelling studies in combination with observational evidences has been so influential in predicting sea breeze front behaviour and the influence of environmental controls on sea breeze circulation structure (e.g. Pielke, 1974, Abbs, 1986, Ado, 1992, Miao et al.,2003, Childs and Raman, 2005,Freitas et al., 2006, Crosman and Horel,2010, Robinson et al, 2013 and Steele et al,2014).

In this study, in order to detect the inland onset and duration of the sea breeze, the basic meteorological parameters including wind direction, wind speed, relative humidity and temperature were first analysed at the Adelaide Airport weather station. As relative humidity is highly temperature dependent, specific humidity was also calculated as a conservative parameter for the analysis of the atmospheric moisture inland flow based on the method described in Foken and Nappo (2008)

The onset of the sea breeze was determined by a sudden change in wind direction

accomplished with almost stable wind speed. More importantly, the intrusion of the cold, moist current can cause a clear temperature decline at the Adelaide Airport. In this study a *temperature decline* refers to a temperature reduction due to sea breeze during a certain time interval. A typical example of a sea breeze day in which the breeze reduces the ambient temperature at the Adelaide Airport is presented in Fig.3 for the summer month of January.

Example of the Method Application on Detecting Sea Breeze Onset at the Adelaide Airport

Detection of Sea Breeze Onset on 25th January 2012

On 25th January 2012, the easterly wind suddenly changes its direction to the south westerly wind around 12:30 (Fig. 3a) accomplished with almost stable wind speed of 11 m/s (Fig. 3b). The wind direction is classified in 8 wind compass points based on the points on Compass Rose (Boardman, 1983) and is shown in Table 4. For example, the wind direction(sea breeze) at 13:30 in the Adelaide Airport is 220 degrees which is between 180 degrees and 270 degrees and is classified as south westerly wind.

The sea breeze onset time, the observed temperature at the onset and the minimum temperature experienced by the sea breeze passage are defined as t_0 ,T_0 and T_{min} respectively (Fig. 3c). Also, dT_{max} is referred to the maximum temperature decline related to the front passage (T_{min}- T_0). In 25th January 2012, the temperature starts declining from 29.2°C (T_0) at 12:30 (t_0) to 25.4°C (T_{min}) at 15:00 at the Adelaide Airport (Fig. 3c). So, dT_{max} of almost 4°C is observed at the Adelaide Airport during the sea breeze front passage . Considering the maximum daily temperature of 35.1 °C recorded at the Kent Town weather station for this day, the 4°C temperature decline by the natural cooling source of sea breeze is much more noticeable. This decline is well consistent with a distinctive rise in specific humidity as much as 2.9g/kg during the same time window (Fig. 3d). More examples of a sea breeze day in which the

breeze reduces the ambient temperature in February, March and December at the Adelaide Airport as well as results of the sea breeze onset detection in the typical sea breeze days are discussed in Chapter 4.

Table 4: Wind direction classification.

Wind Direction(WD)in degrees	Wind Direction Classification
225≤WD≤315	Westerly(W)
180<WD<270	South Westerly(SW)
315<WD<360	North Westerly(NW)
45≤WD≤135	Easterly(E)
135<WD<180	South Easterly(SE)
0<WD<45	North Easterly(NE)
WD=180	Southerly(S)
WD=0 or WD=360	Northerly(N)

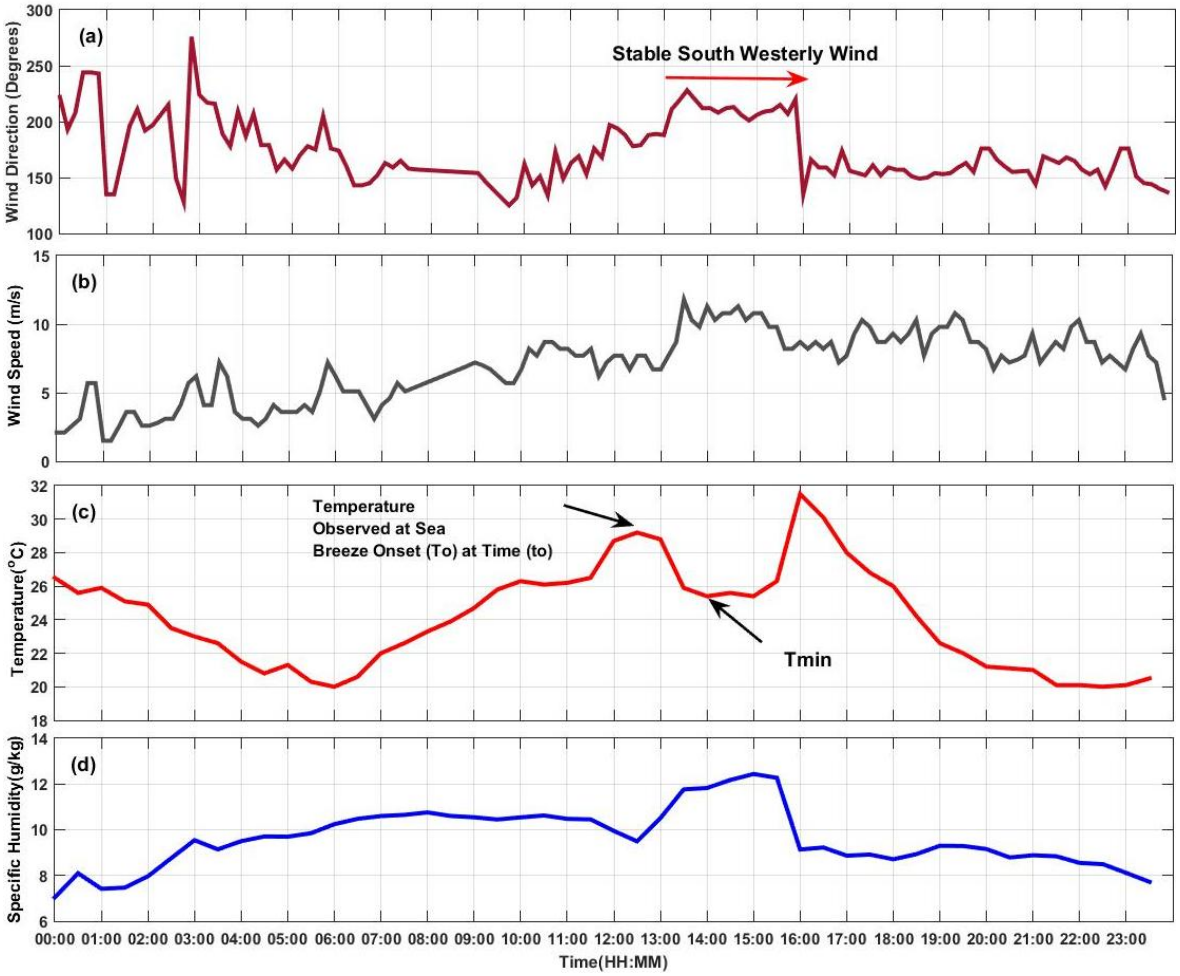

Figure 3: Sea breeze onset detection on 25th January 2012 at the Adelaide Airport (a) Change of wind direction to the stable south westerly wind (b) Stable wind speed during the sea breeze onset (c) The sharp temperature decline after the sea breeze onset (d) The distinct increase in the specific humidity at the onset time.

Sea Breeze Cooling Power

Reference Curves

Base Reference Curves

Considering a day in which the sea breeze could reduce daily temperature by a certain amount (e.g. 4°C in 25th Jan 2012 in the Adelaide Airport), the cooling ability can be quantified by comparing the observed thermal pattern of the day with a simulated one without the sea breeze cooling effect. In fact, we try to estimate how much the temperature could rise if the sea breeze didn't happen in the observed sea breeze day. This is presented in a reference temperature curve. In order to generate the reference curves, the half an hourly observed temperature data of each individual station were selected for each individual months during

the summer months of 2010-2013. Then sea breeze days and the temperature data of rainy and/or cloudy days were removed from the data. In addition, for each individual half an hourly group of the data, percentile analysis was done to detect the unusual extreme high or low temperatures (e.g. heat wave days or the cold front days) and the data placed above 95 percentile or below 5 percentile considered as extreme values. These data weren't counted in the data analysis. The normal distribution of the resulted data were then checked and confirmed.

Finally, the *base reference curves* was generated by applying piece wise linear regression to the scattered half an hourly temperature data. The related scattered plot for the Adelaide Airport station in January and the generated base reference curves are shown in Fig. 4.The scatter plots and the generated base reference curves for February, March and December is presented in Appendix A.

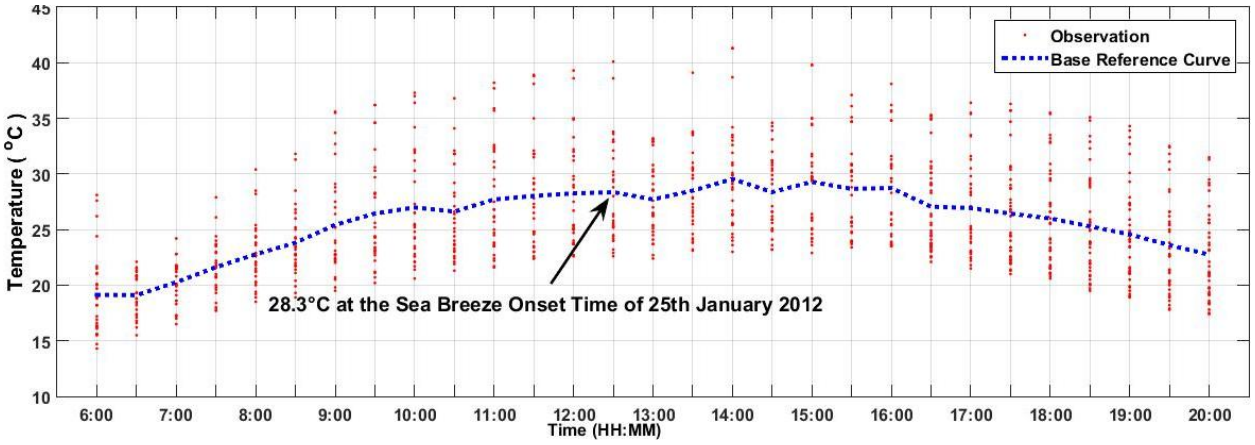

Figure 4: Scattered half an hourly temperature data and the generated base reference curve for the Adelaide Airport station, in January.

Adjusted Reference Curves

For each individual station including Adelaide Airport, Kent Town, Netley, Adelaide CBD and Adelaide parklands a separate reference curve created for each individual summer month. So, twenty reference curves were generated in total. They are the base reference curves and they are considered to be the representative of the diurnal pattern of the temperature change rates in a typical day without the sea breeze occurrence. But, for each single sea breeze day, and during the sea breeze cooling effect, the temperature would decrease to a certain level which could be totally different from the other day, if the sea breeze didn't occur. This is highly dependent on the temperature when the cooling starts (T_0). To adjust the base reference curves to the thermal pattern of a sea breeze day, the temperature of the related base reference curve is shifted to the T_0 of the observed curve of the day. Then the temperature in the shifted reference curve is raised based on the predefined rates of half an hourly temperature change in the related base reference curve. The resulted curve is called the *adjusted reference curve*.

For example, in 25th January 2012, the T_0 is 29.2°C at the sea breeze onset time of 12:30 (Fig. 3c). Considering the base reference curve in January for the Adelaide Airport (Fig. 4), it has the

value of 28.3 °C at 12:30. So, the 28.3 °C at 12:30 in the base reference curve is shifted to 29.2°C (T_0) at 12:30 in the observed curve. Now, the temperature in the shifted reference curve starts rising based on the rates defined in the base reference curve (Fig. 4).

Sea Breeze Cooling Power Calculation

Sea breeze cooling power (SBCP) is defined as the area between the temperature curve of the observed data and the adjusted reference curve from the time at which the observed temperature starts declining (t_0) due to the sea breeze onset up to the time it reaches its first maxima (t_{max}) after the cooling, or the time at which the two curves intersects. It has the unit of °C.min (Equation 1). The presented area for the SBCP in the Adelaide city in Fig. 5a and parklands in Fig. 5b are the examples of the area between the temperature curve of the observed data and the adjusted reference curve when the temperature reaches its t_{max} after the sea breeze cooling. Also, the presented area for the SBCP at the Adelaide Airport in Fig. 5a and Kent Town weather station in Fig. 5b are examples of the area between the temperature curve of the observed data and the adjusted reference curve when the two curves intersects after the sea breeze cooling.

$$SBCP = REF - OBS \qquad (1)$$

where , REF is the integral of the estimated reference curve of temperature versus time and OBS is the integral of the temperature curve of the observed data versus time, both in the unit of °C.min. The REF and OBS are calculated as bellow:

$$REF = \sum_{i=1}^{n} \frac{(T_{ref\,(i-1)} + T_{ref\,(i)}) \times \Delta t}{2} \qquad (2)$$

$$OBS = \sum_{i=1}^{n} \frac{(T_{obs\,(i-1)} + T_{obs\,(i)}) \times \Delta t}{2} \qquad (3)$$

where Δt is the time step at which the data was recorded in the unit of minutes. $T_{ref\,(i)}$ is the

temperature in the reference curve at time t_0+ Δt in the unit of degrees centigrade.

$T_{obs\ (i)}$ is the temperature in the observation curve at time t_0+ Δt in the unit of degrees centigrade. n is the total number of time steps (Δt) between t_0 and t_{max} .

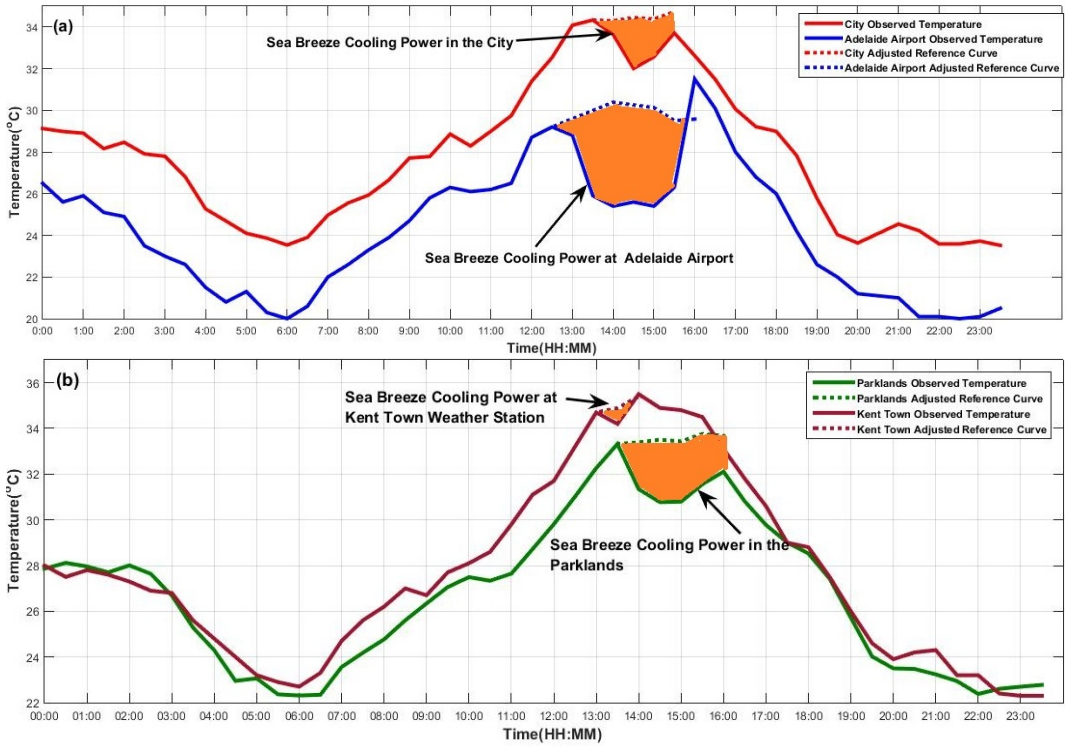

Figure 5: Sea breeze cooling power indicated by the confined area between the adjusted reference curve and the observed curve for (a)the Adelaide Airport station and CBD Stations, (b) the Parklands and Kent Town Weather Station.

Fig. 6 shows the method of calculating the first term of OBS and the forth term of REF for 25th Jan 2012. In the day of 25th Jan 2012, the temperature starts to decline due to the sea breeze onset at 12:30 in the Adelaide Airport. In this case the temporal resolution of the data recording is 30 minutes, which is the representative of Δt in the calculations. As the t_{max} is 14:30, the total number of Δt(s) which is n, gets the value of 4. The confined area by the red trapezoid in Fig. 6 presents the first term of OBS for the selected day. The final OBS is the accumulation of the all calculated trapezoid area for each time step. The same method is applied to calculate REF. The area confined by the gray trapezoid in Fig. 6 shows the forth term

of REF from time step 14:00 to 14:30. Fig. 5 shows the related area to the SBCP after the calculation of the OBS and REF at the Adelaide Airport, City stations, parklands and Kant Town weather station. The estimated SBCP of 645 °C.min,311°C.min, 163 °C.min and 19°C.min for the Adelaide Airport, Adelaide parklands, Kent Town weather station and the CBD, respectively, indicates a significant difference which is a phenomenon discussed in the next section.

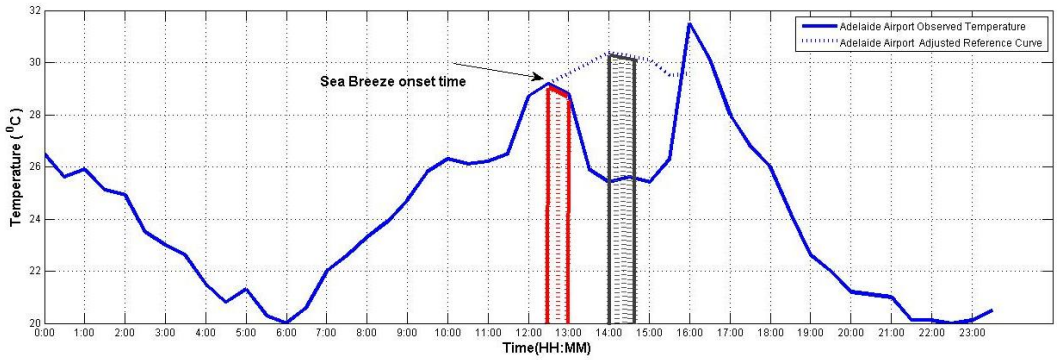

Figure 6: The method used for calculating the first term of OBS and the forth term of REF for 25th Jan 2012. The area confined by the red trapezoid presents the first term of the OBS equation, the time step from onset time (12:30) to the next time step (13:00). The area confined by the gray trapezoid shows the forth term of the REF equation, the time step from 14:00 to 14:30.

4. Results and Discussion

Observation Results of the Typical Sea Breeze Days in the Summer Months

Detection of Sea Breeze Onset on 16th February 2013

Another example of a typical summer day in which the sea breeze helped to relieve from the hot weather is 16th February 2013. The maximum temperature recorded at the Kent Town weather station was 33.8 °C in that day, while a clear temperature decline of almost 4.2°C is observed at the Adelaide Airport during the sea breeze front passage. The easterly wind suddenly changes its direction to the south westerly wind around 10:00 a.m. (Fig. 7a) accomplished with wind speed fluctuating between 5 m/s to 7 m/s (Fig. 7b) at the Adelaide Airport. Also, the temperature starts declining from 32.6°C (T_0) at 9:30 (t_0) to 28.4°C (T_{min}) at 11:30 a.m. (Fig. 7c). So, dT_{max} of almost 4.2°C is observed at the Adelaide Airport during the sea breeze front passage. This decline is well consistent with a distinctive rise in specific humidity as much as 3.88 g/kg during the same time window (Fig. 7d).

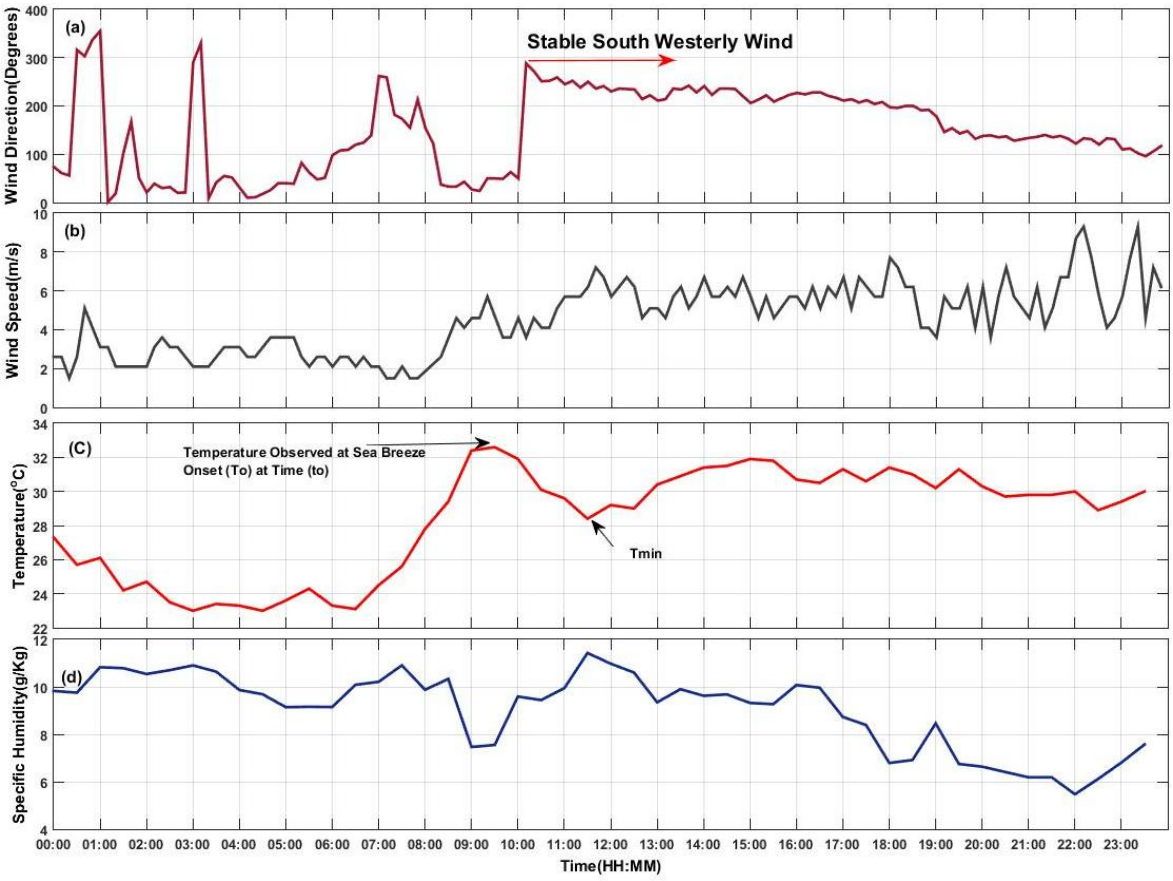

Figure 7: Sea breeze onset detection on 16th February 2013 at the Adelaide Airport (a) Change of wind direction to the stable south westerly wind (b) Wind speed during the sea breeze onset (c) The sharp temperature decline after the sea breeze onset (d) The distinct increase in the specific humidity at the onset time.

Detection of Sea Breeze Onset on 6th March 2011

A significant temperature decline of almost 7.5 °C is detected during the sea breeze passage of the hot summer day of 6th March 2011 with the maximum daily temperature of 34.6 °C recorded at the Kent Town weather station. The easterly wind suddenly changes its direction to the south westerly wind around 12:30 (Fig. 8a) at the Adelaide Airport. The wind speed tends to be almost stable by 15:00 (Fig. 8b). Also, the temperature starts declining from 32.3°C (T_0) at 12:30 (t_0) to 24.8°C (T_{min}) at 13:30 (Fig. 8c). So, dT_{max} of almost 7.5°C is observed at the Adelaide Airport during the sea breeze front passage . This decline is well consistent with a distinctive rise in specific humidity as much as 6 g/kg during the same time window (Fig. 8d).

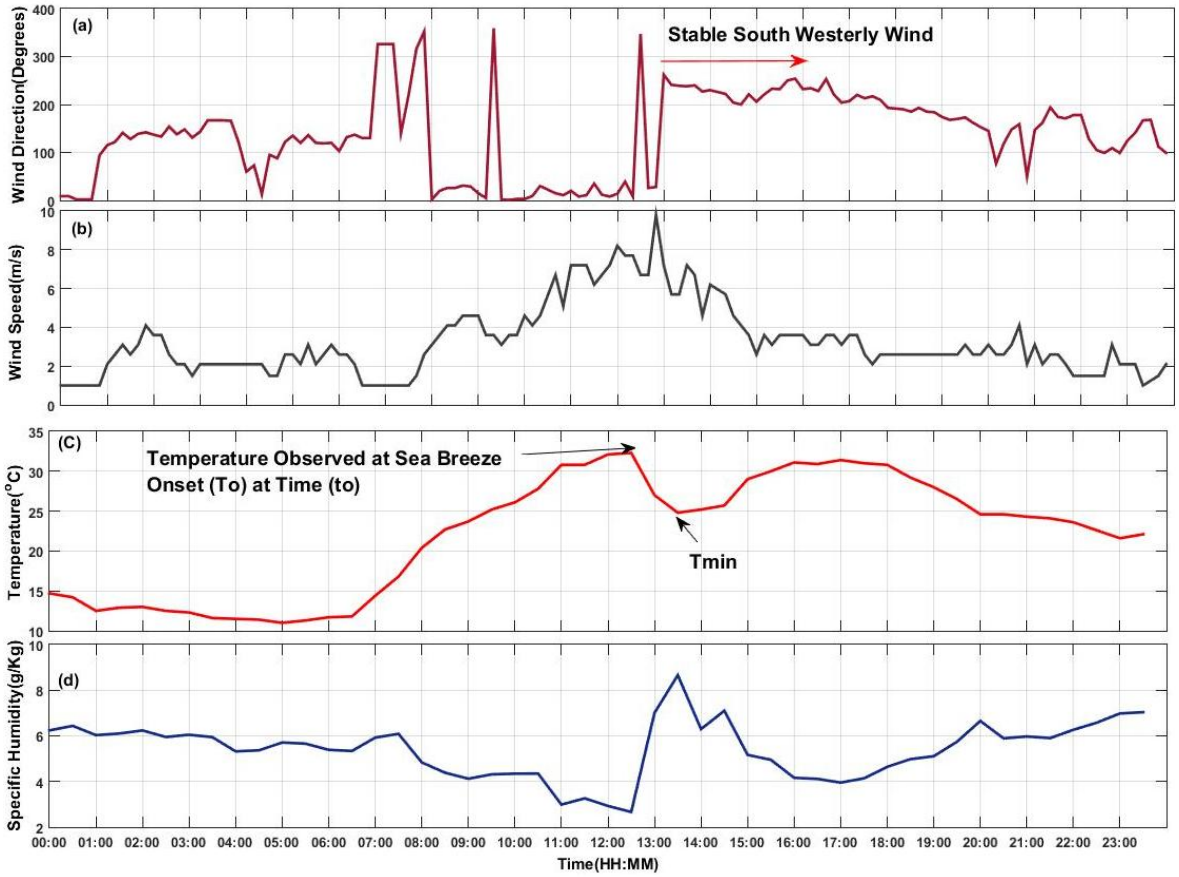

Figure 8: Sea breeze onset detection on 6th March 2011 at the Adelaide Airport (a) Change of wind direction to the stable south westerly wind (b) Wind speed during the sea breeze onset (c) The sharp temperature decline after the sea breeze onset (d) The distinct increase in the specific humidity at the onset time.

Detection of Sea Breeze Onset on 28th December 2011

Another example of a cooling sea breeze day is the 28th December 2011 with the maximum daily temperature of 28.8 °C at the Kent Town Weather station. Although the maximum temperature of this day is not as high as the discussed typical hot summer days, the sea breeze onset and its cooling effect is still detectable at the Adelaide Airport. The easterly wind suddenly changes its direction to the south westerly wind around 11:30 (Fig. 9a) accomplished with almost stable wind speed (Fig. 9b) at the Adelaide Airport. Also, the temperature starts declining from 24.5°C (T_0) at 11:30 a.m. (t_0) to 23°C (T_{min}) at 12:30 (Fig. 9c). So, dT_{max} of almost 1.5°C is observed at the Adelaide Airport during the sea breeze front passage . This decline is well consistent with a distinctive rise in specific humidity as much as 1 g/Kg during the same time window (Fig. 9d).

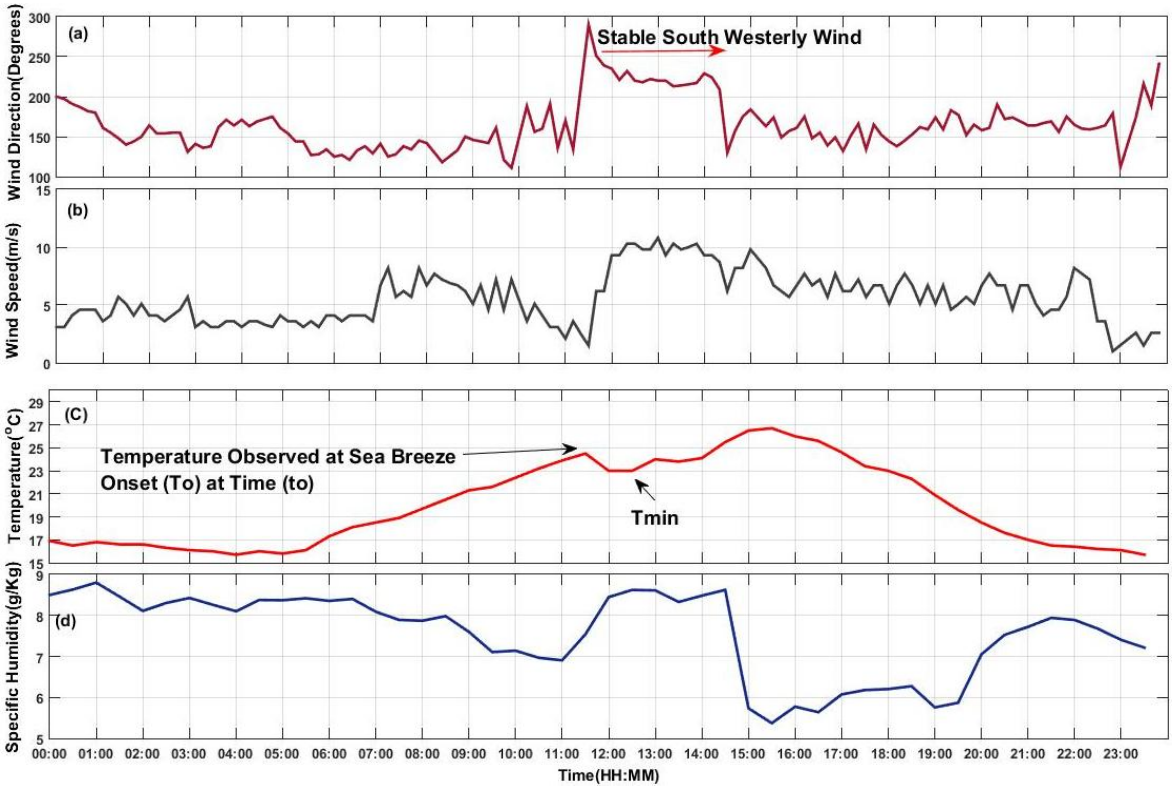

Figure 9: Sea breeze onset detection on 28th December 2011 at the Adelaide Airport (a) Change of wind direction to the stable south westerly wind (b) Stable wind speed during the sea breeze onset (c) The sharp temperature decline after the sea breeze onset (d) The distinct increase in the specific humidity at the onset time.

Cross Checking the Method Findings with Weather Charts Analysis

The examples confirms the findings by Physics and Byron (1975), on the arrival of the continental sea breeze from the southern ocean in the Adelaide shoreline around the noon. The well establishment of the sub-tropical high pressure belt over the southern parts of the continent which created south-easterly gradient winds over the study area in 25th January 2012, 16th February 2013, 6th March 2011 and 28th December 2011 is presented in Fig. 10a, Fig. 10b, Fig. 10c and Fig. 10d respectively. In 25th January 2012, the right side of a high pressure cell with the centre of 1025 (hpa) is over the Adelaide region at 9:30 CST(Fig. 10a), creating south-easterly winds at the Adelaide Airport at that time (Fig. 3a). The wind direction turns to an stable south-westerly wind by the time of sea breeze arrival (Fig.3b). In 16th February 2013, the high pressure cell centre of 1015 (hpa) is almost over the Adelaide region at 9:30 CST (Fig. 10b), creating easterly winds at the Adelaide Airport at that time (Fig. 7a). The

wind direction suddenly changed to south-westerly wind in half an hour as the result of the sea breeze arrival ((Fig. 7b) .The centre of the high pressure cell with the magnitude of 1030 (hpa) already passed over the Adelaide region at 9:30 CST in 6th March 2011 with its left wing still remaining over the area(Fig. 10c), creating northerly winds at the Adelaide Airport at the time (Fig. 8a). The wind direction turns to an stable south-westerly wind by the time of sea breeze arrival (Fig. 8a). In 28th December 2011, the pressure cell over the study area has almost the same situation as in 25th January 2012, with the right side of the high pressure cell over the area at 9:30 CST(Fig. 10d), creating south-easterly winds at the Adelaide Airport at the time which turns to the stable south-westerly wind by the arrival of sea breeze on that day (Fig. 9a). A fair weather, with a clear sky is associated with the area of the high pressure cells in all the typical sea breeze days over the Adelaide region. The maximum temperatures recorded at the Adelaide Airport are 31.5°C, 33.8°C, 33°C and 28.1°C in 25th January 2012, 16th February 2013, 6th March 2011 and 28th December 2011, respectively. In the noticed days, the gradient wind was weak enough to allow the occurrence of the afternoon sea breeze. On the other hand, the land-sea thermal contrast could be totally suppressed by either the dry, hot northerly winds of the heat wave synoptics or prevailing easterly gradient winds (Physics and Byron, 1975).

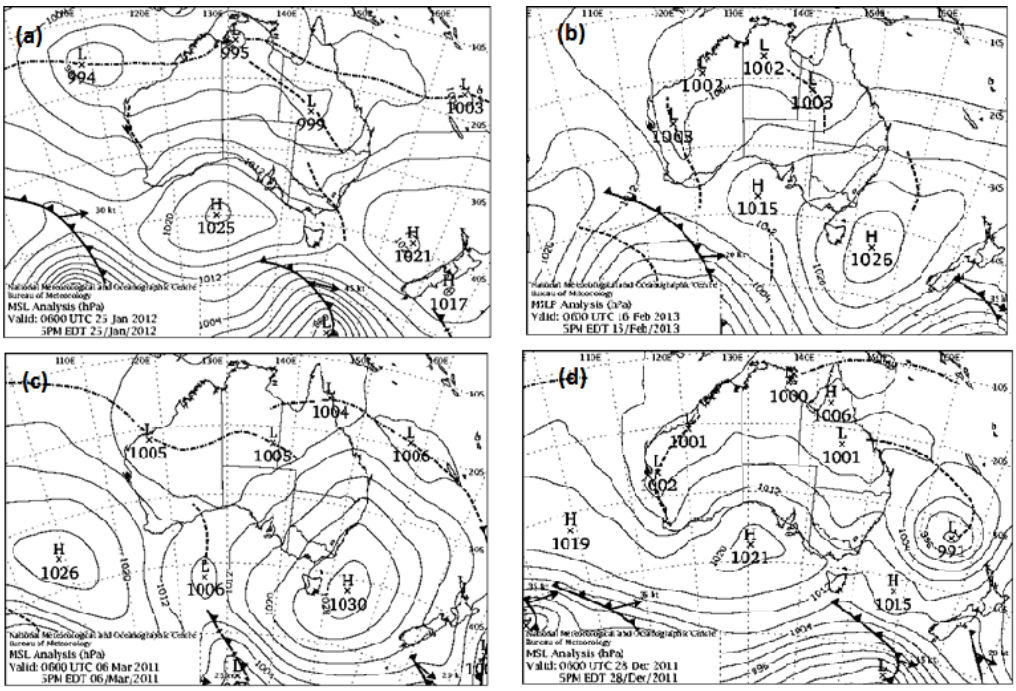

Figure 10: Establishment of the sub-tropical high pressure belt over the southern parts of the continent Accomplished with the south-easterly gradient winds over the study area, (a) on 25th January 2012 (The Australian Bureau of Meteorology, 2017), (b) on 16th February 2013 (The Australian Bureau of Meteorology, 2017),(c) on 6th March 2011 (The Australian Bureau of Meteorology, 2017) and (d) on 28th December 2011 (The Australian Bureau of Meteorology, 2017).

The south easterly gradient wind is followed by the passage of a cold front established with a sudden southerly shift of wind direction and a significant temperature drop in late afternoon of the day. So, analysing the meteorological parameters without looking at the synoptic weather pattern, the weather change of the cold front passage may be considered as sea breeze effect by mistake. To avoid any mis-selection of the sea breeze days, the daily synoptic charts were cross checked with the meteorological data.

In addition, the rainy days and the cloudy days with cloud coverage more than 1 Okta were removed from the analysis. The cloud coverage calculations are summarized in Appendix B.

On the other hand, the sea breeze could occur and/or last to the afternoon when the land experience heat relief from the diurnal temperature decline. Therefore, distinguishing between the purely cooling effect of sea breeze and the afternoon temperature reduction during these time domains of days could be challenging. So, the time window for data analysis is considered

from 7:00 to the time at which the diurnal temperature reaches its maxima. In December and January the maxima occurs around 15:00 central standard time (CST) and around 14:00 CST time in February and March based on half an hourly temperature data from Kent Town weather station.

Temporal Distribution and Frequency of the Sea Breeze Cooling Events

The sea breeze cooling onset can start at any time during the selected time window (early morning to the time of diurnal maximum temperature) in each individual sea breeze day. The duration of the resulted sea breeze cooling varies, from 30 minutes, the finest temporal resolution on the recorded data, to the longer time periods (e.g. 1 hour, 1.5 hour, etc,...). These time periods are called time intervals in this study. In this study, sea breeze cooling in a 30-minute time interval means a temperature decline which lasts at least for 30 minutes due to the sea breeze effect. The temporal distribution of temperature declining magnitude as well as the frequency of their occurrence are analyzed for each individual time interval for all sea breeze days.

Fig. 11 shows the temporal distribution of temperature reduction per half an hour time interval in the Adelaide CBD. In general, a considerably high percentage of the data present cooling rates less than 1°C/ 30 min. Moreover, the frequency of the cooling in 30-minute time interval is significantly higher in the early afternoon compared to the morning time for all four warm months. This could be related to the stronger cross shore temperature difference in the warmer hours of the days.

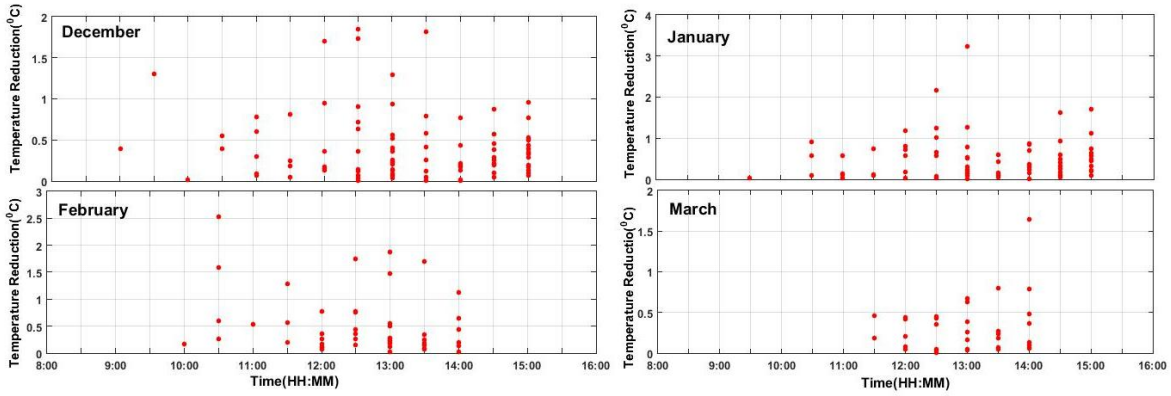

Figure 11: Temporal distribution of temperature reduction per half an hour time interval of sea breeze days in each individual summer month in the Adelaide CBD.

Although the temperature drop starts roughly at the same time, around 10:30, in January, February and December, a delay of one hour to 11:30 is detected in March (Fig. 11). This could reveal the later development of the sufficient land-sea thermal contrast for the sea breeze intrusion into the city in March compared to the rest of the summer months.

Table 5 shows the mean of temperature decline (MTD) and the mean of maximum temperature decline (XTD) in different time intervals analysis for the Adelaide CBD. As the number of the temperature reductions that lasted more than 1.5 hour was quite limited, the results are presented up to 1.5-hour time interval analysis.

Table 5: Mean of temperature decline (MTD) and mean of maximum temperature decline (XTD) in 30 minutes, 1 hour and 1.5 hour time interval in the Adelaide CBD

	30 Minutes Time Interval		1 Hour Time Interval		1.5 Hour Time Interval	
Month	Mean of Temperature Decline(°C)	Mean of Maximum Temperature Decline(°C)	Mean of Temperature Decline(°C)	Mean of Maximum Temperature Decline(°C)	Mean of Temperature Decline(°C)	Mean of Maximum Temperature Decline(°C)
December	0.39	0.89	0.64	0.97	0.68	0.96
January	0.52	0.96	0.84	1.63	0.95	1.42
February	0.53	1.30	1.1	1.80	1.36	2.01
March	0.31	0.74	0.48	0.56	-	-
Mean of Summer Months Temperature Decline	0.44	0.97	0.77	1.24	1.00	1.46

According to Table 5, the mean MTD for all the summer months is as significant as 1 °C in the 1.5-hour time interval in the Adelaide CBD, however February presents the highest MTD and XTD, followed by January, December and March, respectively in all the time intervals. Moreover, the ratio of MDT in 1.5-hour time interval (1°C) to MDT in 30-minute time interval (0.44°C) is 2.27 which could indicate the important role of sea breeze consistency in its power to reduce the ambient air temperature.

In addition, according to Fig. 12a, the average dT_{max} in January, February and December is as significant as almost 1°C in the Adelaide CBD. The average dT_{max} in each month is the mean of all the maximum temperature declines occurred during the sea breeze onsets in the individual month, for which SBCP is calculated. The average of the maximum cooling is reduced by almost 50 percent in March compared to the rest of the summer months. On the other hand, sea breeze cooling occurrence, defined as the number of sea breeze cooling events occurred in a month and for which SBCP is calculated, occurs more frequently in December, followed by January, February and March, respectively (Fig. 12b). This includes 33 percent of the studied days in January and December as well as 25 percent and 22 percent of the studied days in February and March, respectively.

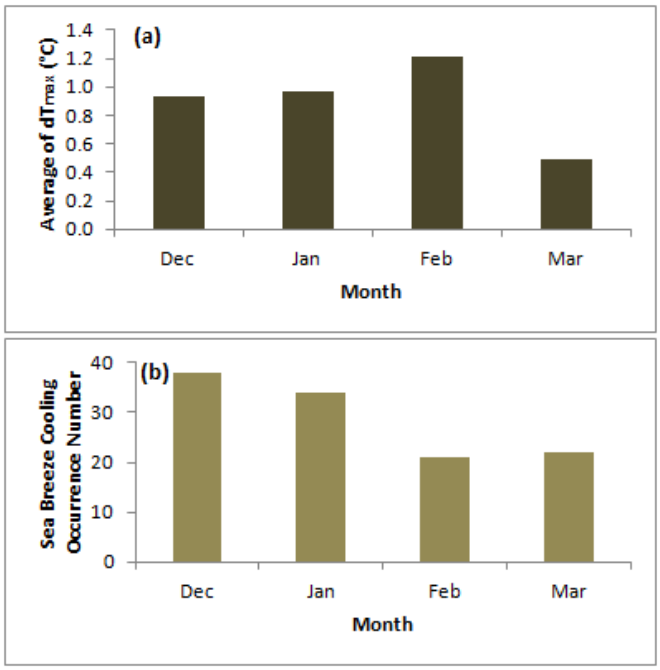

Figure 12: Average of dT $_{max}$ in the summer months 2010-2013 in the Adelaide CBD (a) and, (b) The number of sea breeze cooling occurrence in the summer months 2010-2013 in the Adelaide CBD.

A smaller number of the cooling occurrence in January comparing to December, could be due to the controlling synoptic conditions over the Adelaide region. The common hot, dry northerly winds accomplished with the heat waves play a blocking role against sea breeze development during the month. On the other hand, in the successful sea breeze days of the month, the strong cross shore thermal contrast makes the sea breeze cooling more effective than December, making MTD and XTD of January higher than December in all the examined time intervals (Table 5). Conditions similar to January exist for February. But, in March, although heat waves are still frequent, the significant decline in the number of cooling occurrence is detected. Considering the average of Adelaide CBD temperature for all studied warm months (Table 6), it could be related to the remarkable lower overland temperature in March which weakens the potential development of sea breeze.

Table 6: Average of monthly temperature in the time frame from 8:00 to 20:00 in years between 2010 and 2013 in Adelaide CBD

Month	December	January	February	March
Temperature Average(°C)	26	27	26	23

Sea Breeze Inland Advance Characteristics

The inland advance of the sea breeze cooling events is well accomplished with a drop in the temperature and an increase in the specific humidity. A maximum temperature reduction (dT_{max}) by almost 4°C (Fig. 3c) in conjunction with 2.9 g/kg increase in the specific humidity (Fig. 3d) is well presented after the sea breeze onset on 25th January 2012 at the Adelaide Airport.

Comparing the temperature pattern of the stations during the sea breeze onset on a typical sea breeze day (Fig. 13), the interesting phenomena on the inland cooling effect of the sea breeze is revealed.

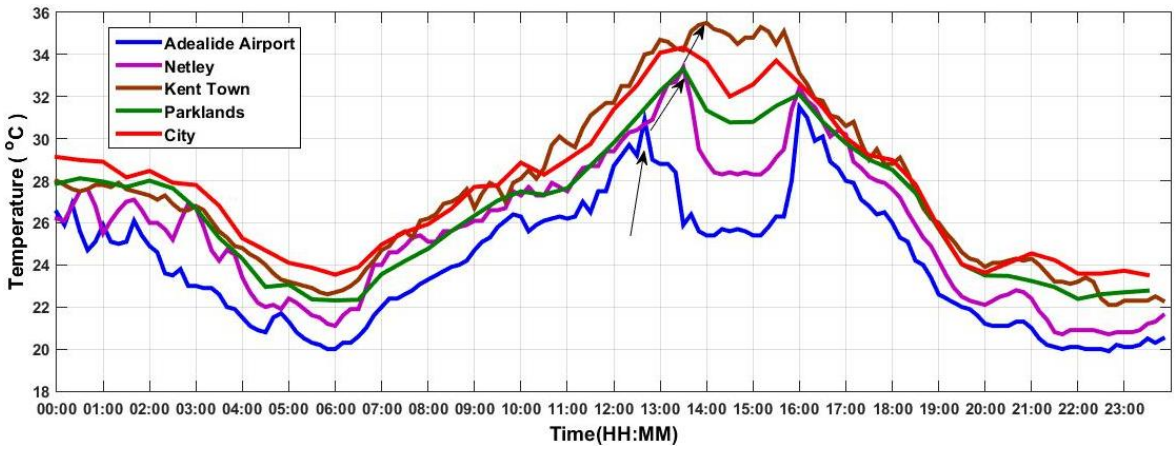

Figure 13: Temporal pattern of temperature change during the inland advance of the sea breeze on 25th of January 2012 in the observation stations.

The black arrows in the Fig. 13 show the sea breeze onset time at the stations. It starts at 12:30 at the Adelaide Airport, then reaches Netley, Parklands and the Adelaide CBD at 13:30 and finally arrives at Kent Town around 14:00. The earlier arrival of the sea breeze at the stations closer to the coast is also found in the specific humidity (q) graph of the Adelaide Airport,

Netley and Kent Town stations (Fig.14).

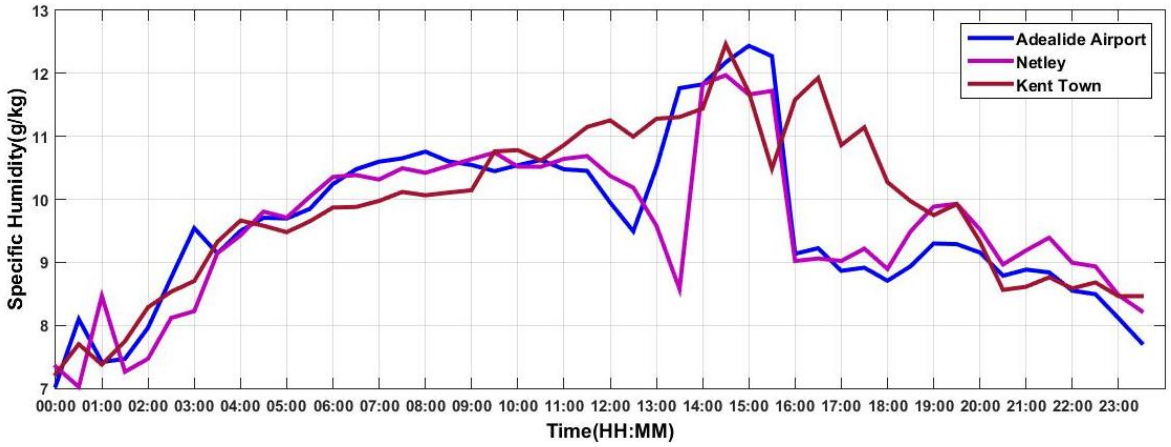

Figure 14: Temporal pattern of specific humidity change during the inland advance of the sea breeze on 25th of January 2012 in the observation stations.

Specific humidity starts increasing around 12:30 at the Adelaide Airport and 13:30 in the Netley station, but shows quite a different pattern at the Kent Town station. This will be further discussed later in this section. The effect of sea breeze advance on temperature and specific humidity pattern is well detected in the other typical sea breeze days discussed in this chapter.

Arrival of sea breeze at the stations of the study area on 16th February 2013 is presented by the arrows in Fig. 15. The arrival time at the Adelaide Airport is 9:30, then it takes half an hour for sea breeze to reach the Netley station at 10:00, and by 11:00 the sea breeze is detected in the CBD and Kent Town stations as well. Moreover, there is a sharp increase in specific humidity started at 9:00 at the Adelaide Airport then it reaches its peak (q_{max}) at 11:30 , where as the significant rise is started at around 11:00 at the Kent Town station (Fig. 16). These times are consistent with t_0 at Adelaide Airport and Kent Town. Also the T_{min} at the Adelaide Airport, Netley and Kent Town is occurred around the time when specific humidity reaches q_{max} at each station.

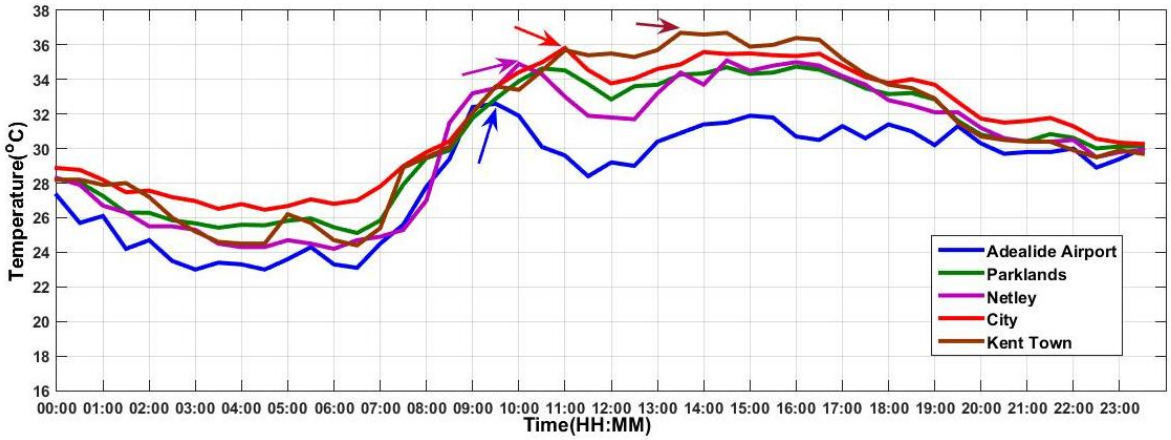

Figure 15: Temporal pattern of temperature change during the inland advance of the sea breeze on 16th February 2013 in the observation stations.

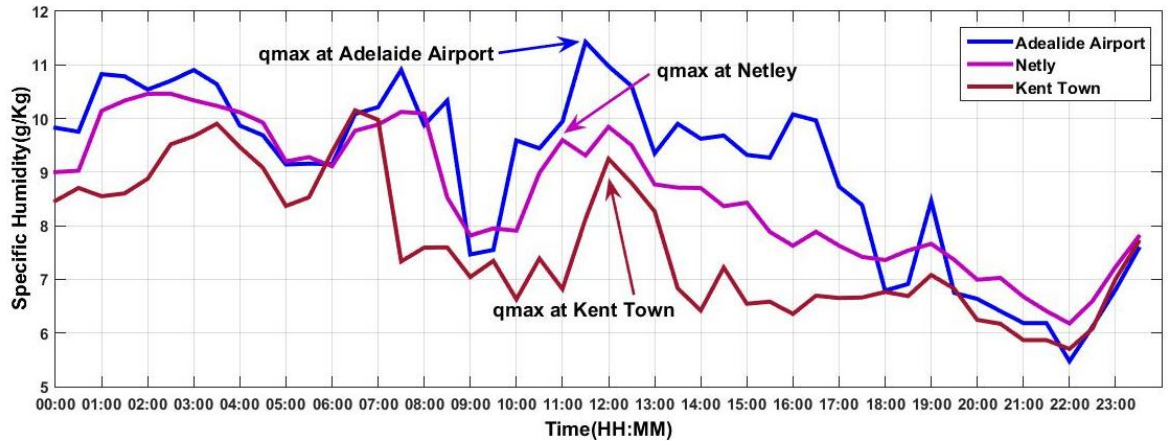

Figure 16: Temporal pattern of specific humidity change during the inland advance of the sea breeze on 16th February 2013 in the observation stations.

The same pattern in the inland advance of sea breeze can be detected in the air temperature and specific humidity graphs of 6th March 2011 (Fig.17 and Fig.18) and 28th December 2011 (Fig.19 and Fig.20).

Sea breeze reaches Adelaide Airport and Netley at 12:30 and 1:00, respectively in 6th March 2011. Half an hour later, at 13:30, sea breeze arrives at parklands and the city stations. Fig. 17 presents the same t_0 for the Adelaide City and Kent Town station. This could reveal that the sea breeze reached the city earlier than the Kent Town station, however its ability to reduce the city temperature is delayed which could be related to the high temperature recorded in the city on that day with a top of 32.4°C.

Moreover, there is a sharp increase in specific humidity started at 12:30 at the Adelaide Airport (Fig. 18) then it reaches its peak (q_{max}) at 13:30, where a significant rise started around 13:00 at the Kent Town station. These times are well consistent with t_0 at Adelaide Airport and Kent Town. Also the T_{min} at the Adelaide Airport is around 13:30 which is the time of q_{max} at the station. Although Netley and Kent experience their T_{min} around 14:30, they receive q_{max} around 13:30 and 14:00, respectively.

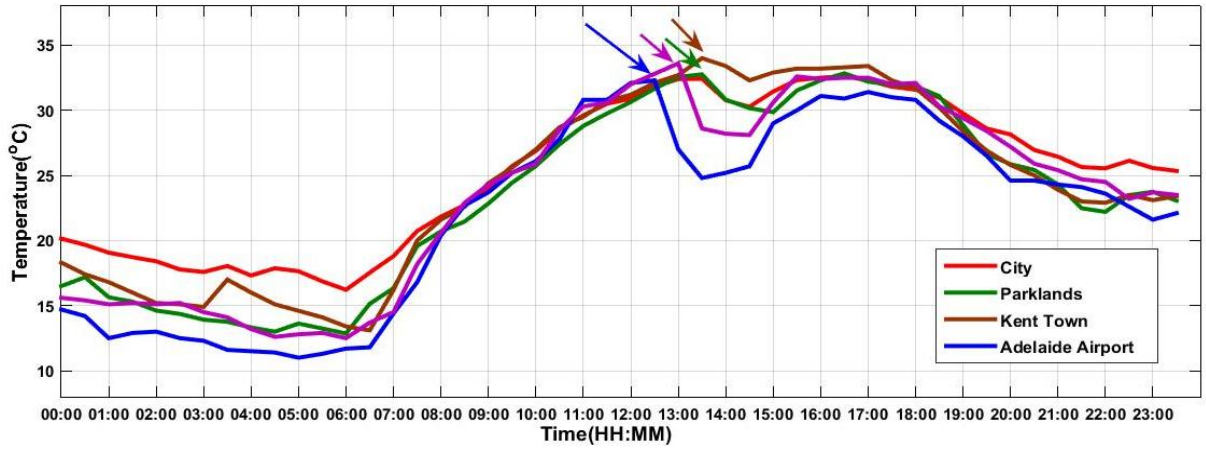

Figure 17: Temporal pattern of temperature change during the inland advance of the sea breeze on 6th March 2011 in the observation stations.

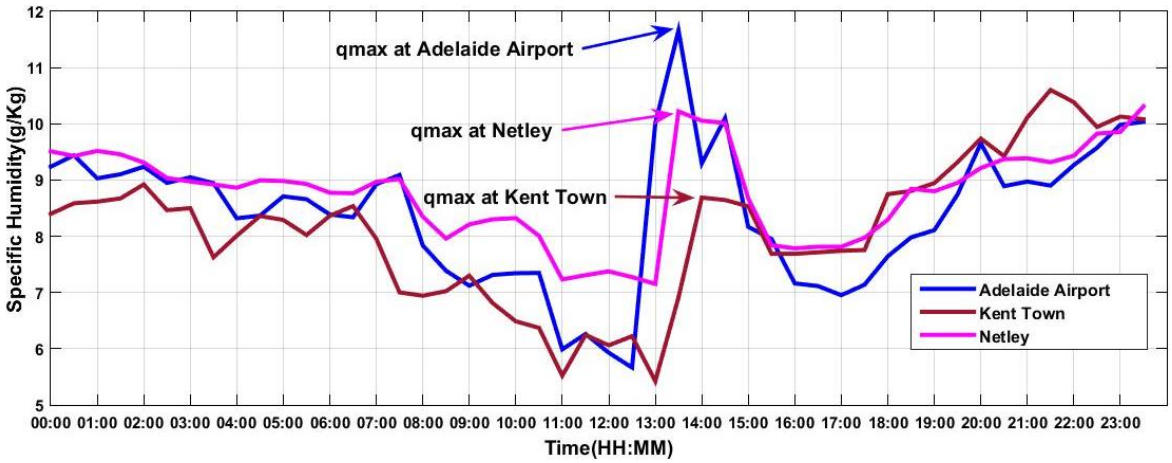

Figure 18: Temporal pattern of specific humidity change during the inland advance of the sea breeze on 6th March 2011 in the observation stations.

On 28th of December 2011, Adelaide airport and Netley experience the sea breeze cooling at 11:30 and 12:00, respectively (Fig. 19). The temperature decline starts at 12:30 at parklands and city stations as well as Kent Town (Fig. 19). Moreover, at Adelaide Airport, T_{min} is

experienced at 12:00 and it lasts for half an hour when specific humidity reaches q_{max} (Fig. 20). Also, Netley and Kent Town have their T_{min} at 12:30 and 13:00, respectively, when q_{max} happens at the stations (Fig. 20).

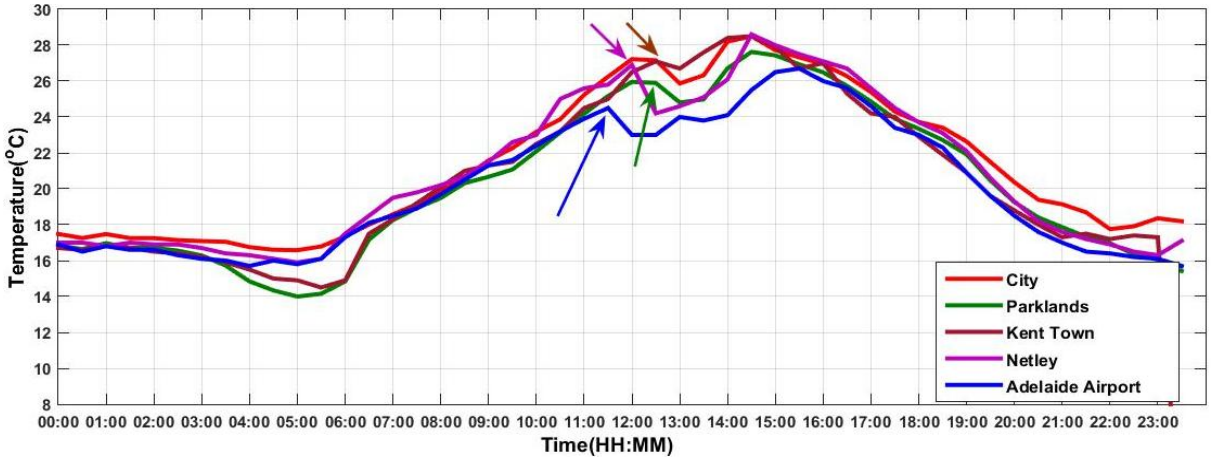

Figure 19: Temporal pattern of Temperature change during the inland advance of the sea breeze on 28th December 2011 in the observation stations.

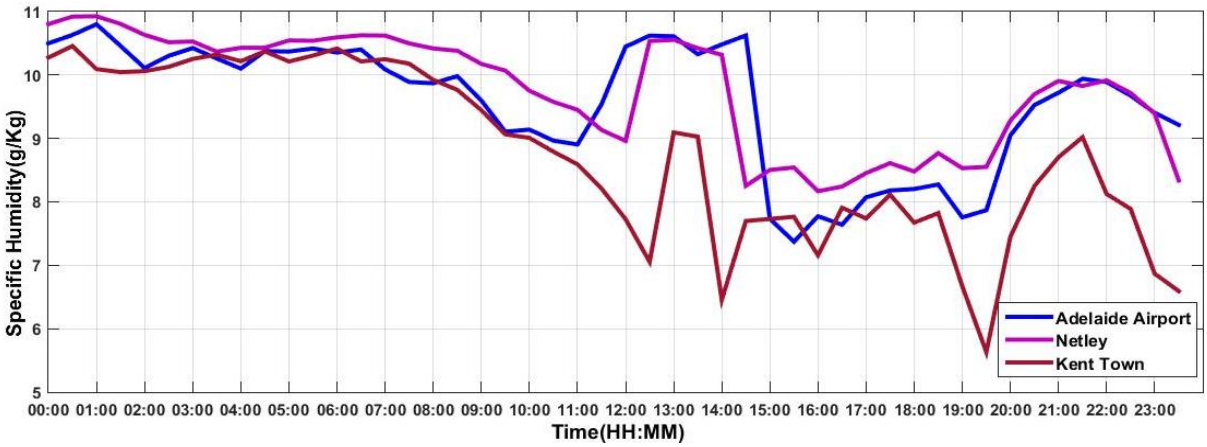

Figure 20: : Temporal pattern of specific humidity during the inland advance of the sea breeze on 28th December 2011 at the observation stations.

In addition, in all the discussed typical sea breeze days, Adelaide Airport shows significantly lower T_0 than the other stations further away from the coast line. Also q_{max} is higher at the Adelaide Airport and Netley comparing to the Kent Town station. The closer to the shoreline, the lower T_0 and the higher q_{max} is observed at the stations. For example, on 25th January 2012,

16th February 2013 and 6th March 2011, the Kent Town station experiences 6.3°C, 3.1°C and 1.7°C higher temperature than the Adelaide Airport, respectively. The elevation difference between the stations couldn't result in the significant temperature difference between the stations as the Kent Town station is elevated 46 meter more than the Adelaide Airport.

However the experienced q_{max} at the Kent Town station are 3 g/kg and 2.2 g/kg lower than Adelaide Airport on 16th February 2013 and 6th March 2011, respectively, there is not a significant difference between the q_{max} of Kent Town and Airport on 25th January 2012.

The inland increase in the T_0 over the study area on 25th January 2012 is well presented in the colour map of Fig. 21a. The same pattern is detected for T_{min} Fig. 21b. It is interesting that, although T_{min} in the Adelaide Airport, Netley and the Parklands happens around 15:00, the Kent Town and city observes T_{min} around 14:30. In addition, there is a decline in dT_{max} at the stations (Fig. 21c).The amount of ΔT in the Kent Town station is well consistent with the gentle increase in the specific humidity graph during the sea breeze passage from the site (Fig. 14).

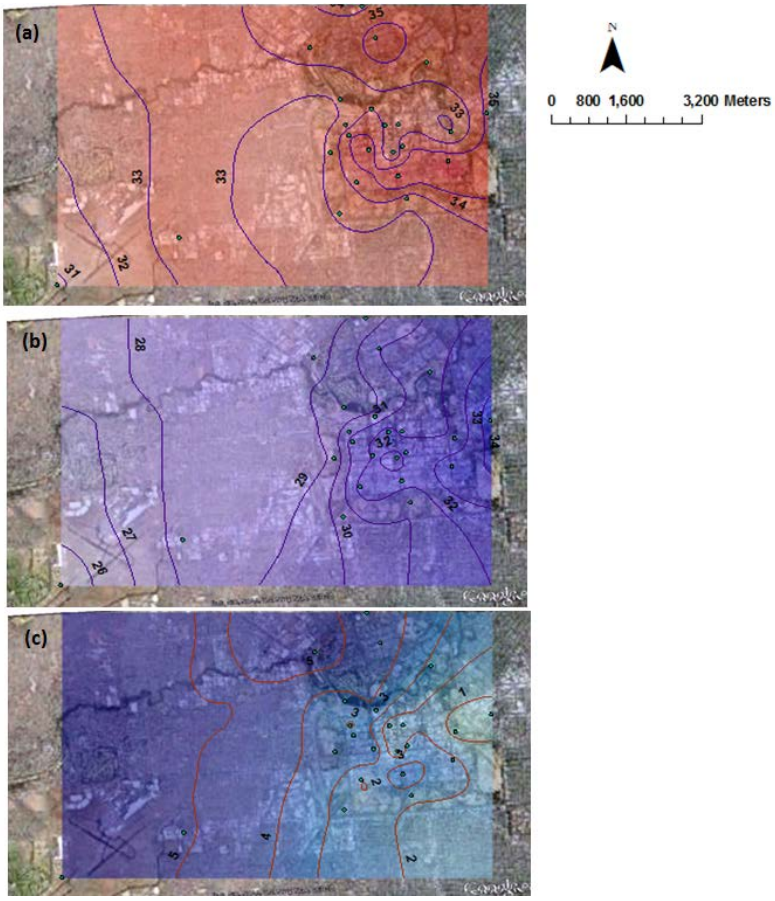

Figure 21: Spatial distribution of T_0 during the sea breeze day of 25th January 2012 (a), Spatial distribution of T_{min} during the sea breeze day of 25th January 2012 (b), Spatial distribution of dT during the sea breeze day of 25th January 2012 (c).

In the case of the Kent Town station, its further proximity from the coast comparing to the other stations, the sea breeze stagnation in the CBD due to the Heat Island Circulation (HIC) as well as the CBD urban frictional drag [e.g., Yoshikado et al., 1992; Cenedese et al., 2003; Freitas et al., 2007; Sashiyama et al., 2014], could be the reasons for the delay of the sea breeze arrival to the Kent Town and the reduction of ΔT received by the station.

In the Adelaide CBD, the elevated sensible heat flux in the area resulted from the Urban Heat Island (UHI) phenomenon, could reduce the cooling efficiency of the sea breeze. Although based on the results of the study by (Vinodkumar et al. 2012), the intense UHI is mostly observed in summer nights, but the less intense UHI could be also detected during the daytime. The higher daytime temperature in the CBD is well presented in Fig. 13, Fig. 15, Fig.17 and Fig. 19. In addition to the thermal influence of the city on the sea breeze cooling effect, the

blockage of the wind flow by the urban morphology may restricts some urban areas from receiving the cool, moist sea breeze. This effect is considered to be analysed in the future studies in this area.

Spatial and Temporal Patterns of the Sea Breeze Cooling Power

The *Sea Breeze Cooling Power (SBCP)* is estimated for each individual sea breeze cooling event in the summer months of 2010-2013 for each of the individual stations using the method described in the chapter 3.Then *Cumulative Sea Breeze Cooling Power (CSBCP)* is calculated by the summation of all the estimated SBCP in the summer months.

As Fig. 22a presents, the CSBCP shows a declining trend during its inland advance for all summer months with the Adelaide Airport receiving the highest and the Kent Town station the lowest CSBCP.

In general, the cumulative sea breeze cooling power of 62577 °C.min in the Adelaide Airport is 4.1, 2.9, 2.4 and 1.2 times its amount in Kent Town, Adelaide City, Adelaide Parklands and the Netley station, respectively, in the examined summer. Moreover, the CSBCP in Netley is distinctively close to the CSBCP in the Adelaide Airport with a considerable difference to the rest of the stations in all the summer months (Fig. 22a). The results are consistent with the findings of the cooling event on 25th Jan 2012 (Fig. 5). Considering the coastal distance of the stations in the study area (Table 3), in general, the mean of cumulative sea breeze cooling power at the coastal stations (Netley and Adelaide Airport) is 2.7 times its magnitude at the rest of the stations (Fig. 22b).

The ratio of the mean CSBCP in the coastal stations to the non-coastal stations is called *CSBCP ratio* in this study. The CSBCP ratio in January, February, March and December are 3.9, 2.1, 4.4 and 2, respectively. Therefore, the CSBCP ratio is almost the same in January and March and is

twice as the ratio in February and December. In March, the high CSBCP ratio could be the result of the weaker land-shore thermal contrast comparing to the other summer months, so the ability of the established sea breeze to transfer its cooling power to inland areas is less than the other summer months. In January, the predominant high speed northerly winds may reduce the ability of the inland advance of the sea breeze resulting into the high CSBCP ratio.

Moreover, as sea breeze advances inland, its thermal characteristics changes due to the heat exchange with the ambient environment which could reduce the cooling ability of the sea breeze, leading to the significant difference between the CSBCP of the coastal stations and the Adelaide CBD and the Kent Town station. The mentioned significant difference also reveals the possible effect of urban frictional drag and HIC on sea breeze intrusion into the city resulted from the blockage of the cool air in some city locations as well as cooling stagnation in the city. In addition, the coastal distance accomplished with an increase in the surface elevation could be the other reasons behind the phenomenon. However, the latter seems to have an ignorable effect as the amount of the elevation difference of maximum 60 meters is significantly less than the scale of the common the sea breeze circulation.

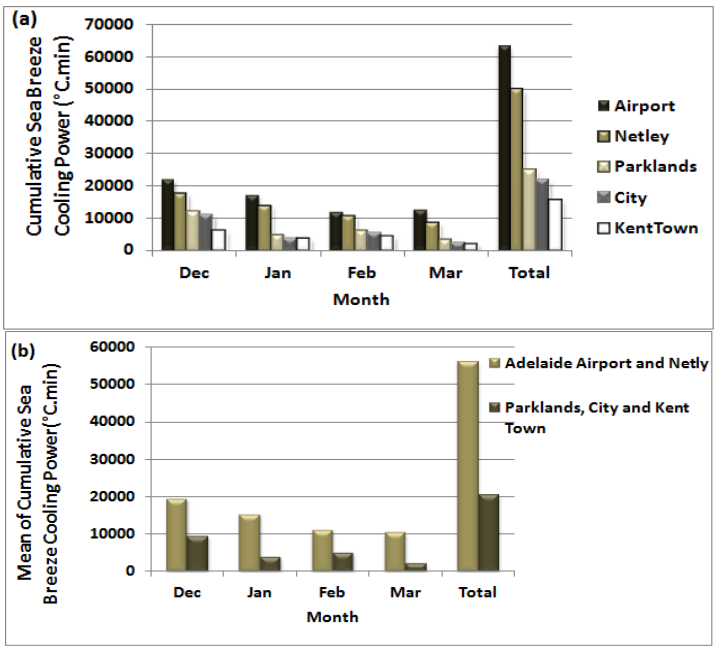

Figure 22: Cumulative sea breeze cooling power at the observation stations of the study area in the summer months between 2010 and 2013 (a), Mean of Cumulative Sea Breeze Cooling Power at the Coastal Stations (Adelaide Airport and Netley) and Non-Coastal Stations (Parklands, City and Kent Town) (b).

On the other hand, the city stations show a slightly different monthly order of CSBCP. Although in December and March the CBD receives the highest and the lowest CSBCP, but February shows higher CSBCP than January (Fig. 22a). It shows that although the frequency of the cooling events in the Adelaide CBD is higher in January than February (Fig. 12b), but the ability of the sea breeze to reduce the reference temperature is higher in February than January.

Table 7 presents mean of SBCP in each individual summer months. Also the last column of Table 7 shows mean of SBCP in the whole examined summer. Fig. 23, shows the rate of SBCP mean change during the sea breeze inland advance based on the data of Table 7. The horizontal axis, is the coastal distance of the stations. The coastal distance of centre of the city, the Victoria Sq, is considered as the representative of the coastal distance of the Adelaide CBD and the parklands. The vertical axis is the mean of SBCP for each individual station.

In general, the SBCP decreases with the sea breeze inland intrusion. In average, the decline rate is estimated to be 45.5°C.min/km in the examined summer period (Fig. 23a). This result

indicates that the sea breeze cooling power disappears at about 13.8 km orthogonal distance from the coast.

Table 7: Mean of SBCP in each individual summer months and all examined summer months between 2010 and 2013 in the study area.

	January SBCP (°C.min)	February SBCP (°C.min)	March SBCP (°C.min)	December SBCP (°C.min)	All Examined Summer Months
Adelaide Airport	**512.1**	**538.8**	**596.9**	**657.0**	**576.2**
Netley	**413.7**	**471.1**	**437.9**	**509.5**	**458.1**
CBD and Parklands	**112.3**	**259.9**	**132.2**	**317.9**	**205.6**
Kent Town	**112**	**208.3**	**90.7**	**182.3**	**148.3**
Study area	**287.5**	**369.5**	**314.4**	**416.7**	**347**

Although the decreasing rates aren't the same for all the summer months (Fig. 23b), but January and December present almost the same rate with a difference of just 1.35 °C.min/km.

On the other hand the mean of SBCP in December is 145 °C.min more than its amount in January which makes the intrusion ability of the sea breeze about 2.5 km more than January (Fig. 23c). The highest decline rate difference is found between March and February by 16.13 °C.min/km. This is well consistent with the findings in Table 5, in which February presents the highest MTD and XTD and then January, December and March, respectively, in all the time intervals. Moreover, the minimum sea breeze advance capability is found for March (Fig. 23c) due to its higher decline rate in SBCP (Fig. 23b).

In general, the sea breeze inland intrusion has its highest value in February as 16.5 km which is almost 4 km longer than its minimum value in March (Fig. 23c). The comparison between the daily SBCP decline rate of the examined typical sea breeze days of the study and the maximum inland advance of sea breeze in each day confirms this finding. It shows the maximum inland advance of the sea breeze occurred in 16th February 2013 by 14.2 km followed by 13.5 km, 12.1 km and 11.4 km in 25th January 2012, 6th March 2011 and 28th December 2011, respectively (Fig. 23d). These results are well consistent with the finding of CSBCP ratio (Fig. 20b) and could be related to the characteristics of sea breeze direction (SBD) and sea breeze speed (SBS) in each individual summer month.

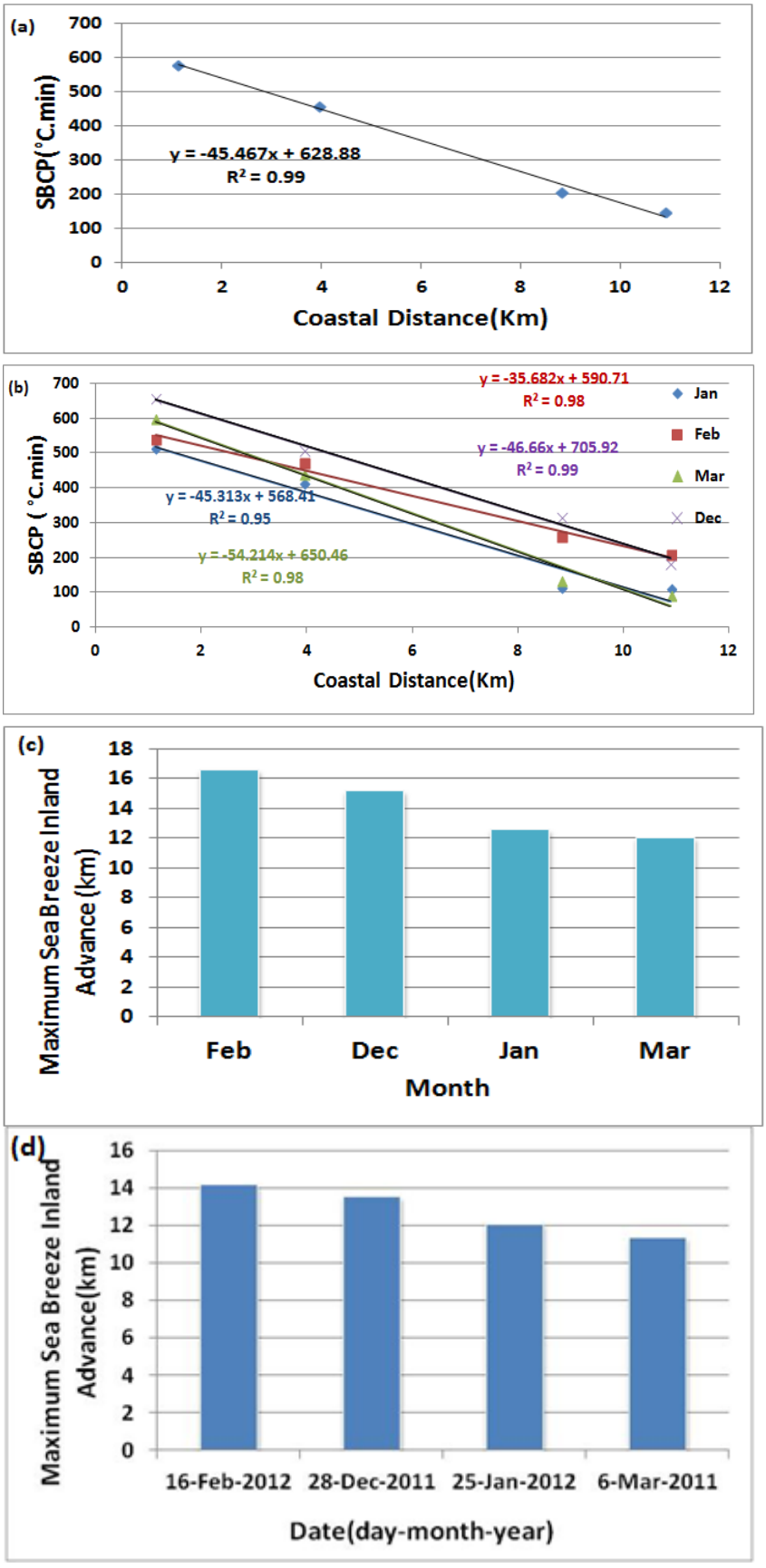

Figure 23: Rate of sea breeze cooling power mean change during the sea breeze inland advance in the all examined summer months (a), Rate of sea breeze cooling power change during its maximum inland advance in each individual summer month (b),Maximum sea breeze inland advance in the studied summer months(c), Maximum sea breeze inland advance in the typical sea breeze days of the study (d).

The sea breeze speed (SBS) and sea breeze direction (SBD) is analyses in all the examined sea breeze days in the time intervals when the sea breeze cooling power is calculated. The high resolution, wind data from the Adelaide Airport is used for the analysis.

The ratio of the number of westerly(W), south westerly(SW) and north westerly(NW) wind data to the total number of the wind direction data in the SBCP time interval of sea breeze days is calculated and presented in Fig. 24a.

In general, more than 50% of the SBD is from west in all the examined summer months (Fig. 24a). Before analysing the wind direction data, the hypothesis was, the more intrusion of sea breeze in a month, the higher westerly sea breeze wind components in the month is detected, resulting into more orthogonal inland movement of sea breeze.

According to Fig. 24a, except in March, sea breezes have more westerly direction in February, followed by December and January, respectively which confirms the hypothesis. In March, although the percentage of westerly sea breezes is higher than the other months, but the percentage of SW sea breezes is almost 12% lower than its average value in the other months. The significant low ratio of south westerly sea breezes which take the cool, moist air over southern ocean over the land could compensate the higher ratio of westerly winds in this comparing to the other months.

Moreover, there is no significant difference between the westerly sea breeze speed between the summer months, however the average speed of south westerly sea breezes in March is 0.8 m/s lower than its average value in the other months.

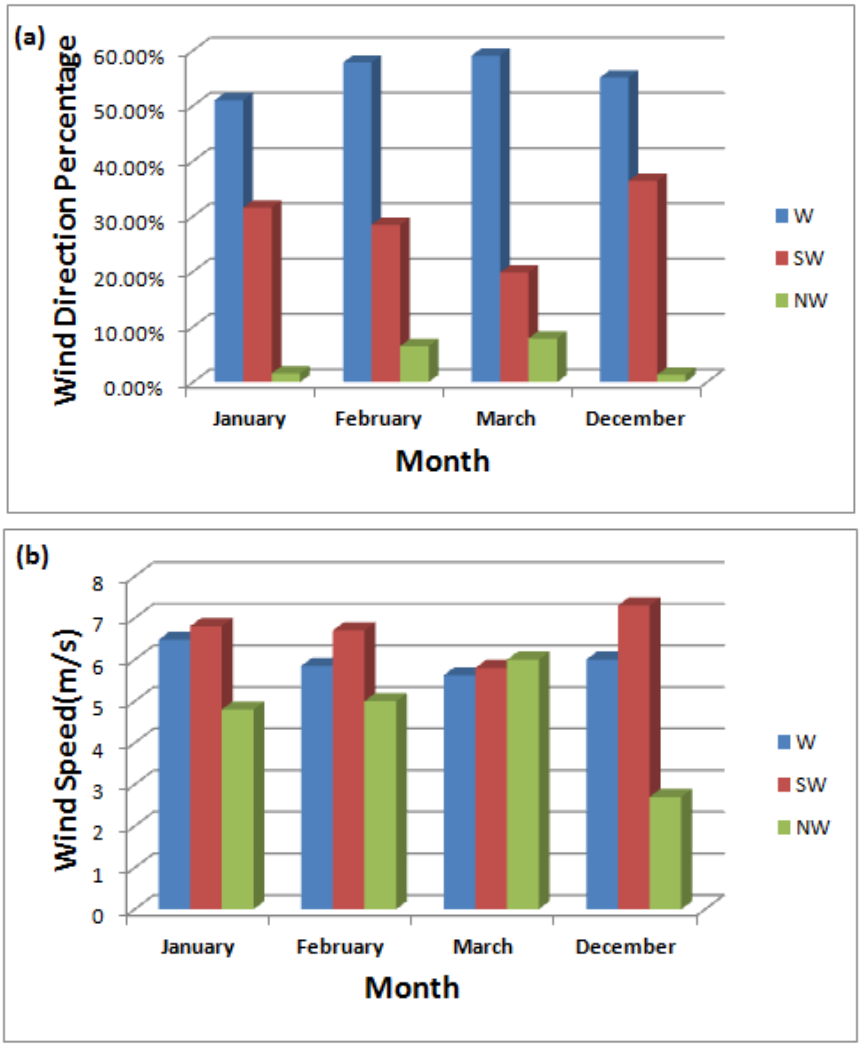

Figure 24: The ratio of westerly, south westerly and north westerly sea breezes to the total number of sea breeze wind direction data in the examines sea breeze days, in the time interval of calculating sea breeze cooling power (a), the average of westerly, south westerly and north westerly sea breeze speed in the examined sea breeze days.

5. Conclusions

The sea breeze onset evolution and its effect on the thermal environment during its advance to the Adelaide CBD were examined during the summer months between 2010 and 2013. Statistical analysis applied on the meteorological data in high spatial and temporal resolution. A clear change in wind direction accomplished with a distinctive rise in specific humidity and almost stable wind speed was detected at the time of the sea breeze onset which can cause a clear temperature decline depending on its strength.

In all the time intervals (e.g. 1 hour, 1.5 hour, etc,...), February presents the highest Mean Temperature Decline (MTD) and Maximum of Mean Temperature Decline (XTD), and then January, December and March, respectively. Moreover, in the all summer months except March, the average of dT_{max} is almost as significant as 1°C in the 1.5-hour time interval in the Adelaide CBD.

On the other hand, the number of the sea breeze cooling occurrence shows is highest in December and then January, February and March, respectively. The same order is found in the monthly amount of CSBCP as well. This could be related to the controlling role of the prevailing synoptic condition on the sea breeze development.

Moreover, closer the stations to the coast, the earlier onset of the sea breeze, the lower T_0 and T_{min} and the higher dT_{max} were found at the stations. In the Adelaide CBD, the elevated sensible heat flux in the area resulted from the Urban Heat Island (UHI) phenomenon in addition to the blockage of the wind flow by the urban morphology may restricts some city areas from receiving the cool, moist sea breeze. This could also be related to the declining trend found in the SBCP during the cool air inland advance in all the summer months with a significant difference detected between the SBCP of the Adelaide Airport and the Adelaide CBD.

In general, the cumulative sea breeze cooling power in the Adelaide Airport is 4.1, 2.9, 2.5 and 1.2 time its amount at Kent Town, Adelaide City, Adelaide Parklands and the Netley station respectively in all the summer months.

The CSBCP ratio has almost the same value in January and March which is twice of the ratio value in December and February. This could be related to the establishment of the weaker sea breeze due to the less strength in the land-shore thermal contrast in March comparing to the rest of the summer months. Also, the inland advance of the sea breeze could be restricted by the predominant high speed northerly wind lead to the resulted high CSBCP ratio in this month.

The cooling stagnation and/or the cooling blockage in some city areas due to the urban frictional drag and HIC could be the other reason making the CSBCP of the coastal stations significantly higher than the CBD stations. The interaction of urban morphology and sea breeze is considered for the future studies in the study area.

The decline rate of SBCP during the sea breeze intrusion, is estimated to be 45.5 °C.min/km on average for all summer months. On average, the sea breeze is estimated to completely lose its cooling power at about 13.8 km in orthogonal distance from the coast, however, in February it could advance as far as 16.5 km inland.

The higher value of the sea breeze orthogonal inland advance in February could be related to the higher percentage of westerly and south westerly sea breezes in this month comparing to the other summer months. On the other hand, the minimum intrusion of sea breeze in March could be related to the lower percentage of south westerly sea breezes with lower speed comparing to the other examined months.

Extensive numerical and analytical studies is recommended to analyse the effect of synoptic wind pattern on sea breeze circulation and local climate of the Adelaide CBD. Numerical

modelling studies are needed to analyse the cooling effect of the sea breeze after the mentioned threshold time in the study to avoid any underestimations of afternoon sea breeze cooling power which is discussed in the next section. Moreover, annual comparison of SBCP in the summer months over a long time period is recommended for future studies to explore the possible effect of climate change on the sea breeze cooling power over the study area.

Appendix A: The scatter plots and the generated base reference curves in February, March and December for Adelaide Airport

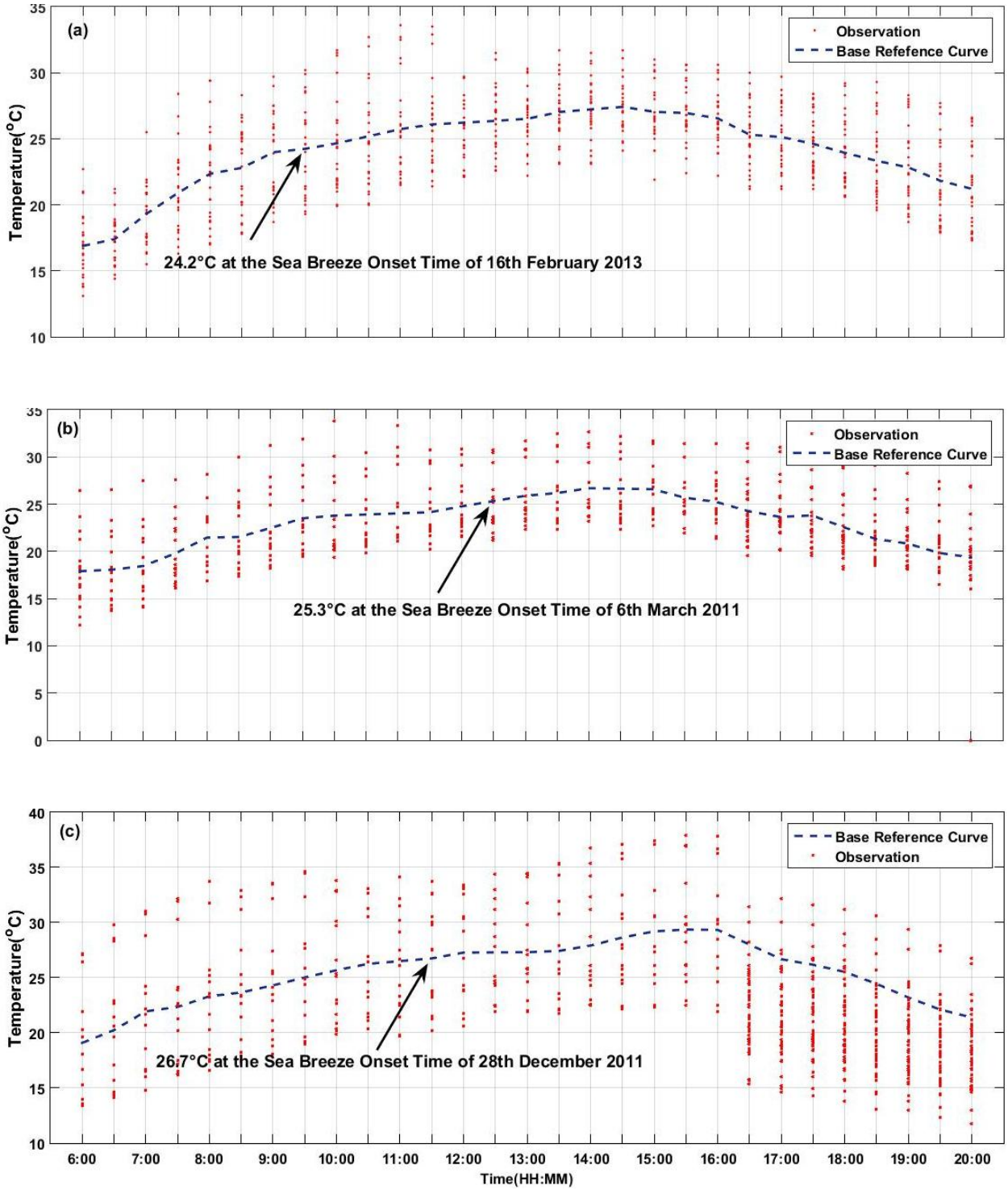

Scattered half an hourly temperature data and the generated base reference curve for the Adelaide Airport station, in February(a), March(b) and December(c).

Appendix B: The Method of Cloud Coverage Calculation in the Study Area

The observed cloud data in the Adelaide Airport was used as it is central to the Adelaide urban area. The data is provided in three main groups, upper level, middle level and lower level clouds. Although the lower level cloud coverage has the most effect on the climate of the study area, but sometimes the middle and/or upper level cloud have greater coverage or is low enough to affect the local climate. Addition of the three cloud coverage is not appropriate as it results into the Oktas greater than 8. So it doesn't provide an accurate measurement for cloud group overlap estimation. A single value that represented the cloud cover was obtained using the below Equation :

$$C_{cov} = 1 - ((1 - C_{L1}) \times (1 - C_{L2}) \times \ldots \times (1 - C_{Ln}))$$

where C_{cov} is the cloud cover and CL1,CL2,CLn are the cloud amounts (eights) in each of the n levels (Kent, 2010).

This equation combines several layers of cloud into one representative value for the fraction of sky covered with cloud, with 0 representing clear skies and 1 representing overcast conditions. Oktas were then identified by binning certain fractions into eighths, for example 1 Okta is assigned to fractions between 0 and 0.125.

Bibliography

Abbs, D. (1986). Sea-Breeze Interactions along a Concave Coastline in Southern Australia: Observations and Numerical Modeling Study. *Monthly Weather Review*, 114(5), pp.831-848.

Acero, J. A., Arrizabalaga, J., Kupski, S. & Katzschner, L. 2013. Urban heat island in a coastal urban area in northern Spain. *Theoretical and applied climatology,* 113**,** 137-154.

Ado, H. Y. 1992. Numerical study of the daytime urban effect and its interaction with the sea breeze. *Journal of Applied Meteorology,* 31**,** 1146-1164.

Alcoforado, M.-J., Andrade, H., Lopes, A. & Vasoconcelos, J. 2009. Application of climatic guidelines to urban planning: the example of Lisbon (Portugal). *Landscape and Urban Planning,* 90**,** 56-65.

Arrillaga, J., Yagüe, C., Sastre, M. and Román-Cascón, C. (2016). A characterisation of sea-breeze events in the eastern Cantabrian coast (Spain) from observational data and WRF simulations. *Atmospheric Research*, 181, pp.265-280.

Ashie, Y., Hirano, K. & Kono, T. Effects of sea breeze on thermal environment as a measure against Tokyo's urban heat island. The Seventh International Conference on Urban Climate, Yokohama, Japan, 2009.

Abs.gov.au. (2016). *3218.0 - Regional Population Growth, Australia, 2012-13*. [online] Available at: http://www.abs.gov.au/ausstats/abs@.nsf/Products/3218.0~2012-13~Main+Features~Main+Features?OpenDocument#PARALINK2 [Accessed 23 Dec. 2014].

Boardman, D. (1983). *Graphicacy and geography teaching*. 1st ed. London: Croom Helm, p.41.

Bom.gov.au. (2017). *Monthly Rainfall - 023090 - Bureau of Meteorology*. [online] Available at:

http://www.bom.gov.au/jsp/ncc/cdio/weatherData/av?p_nccObsCode=139&p_display_type=dataFile&p_startYear=&p_c=&p_stn_num=023090 [Accessed 5 May 2017].

Bom.gov.au. (2017). [online] Available at: http://www.bom.gov.au/cgi-bin/charts/charts.view.pl?idcode=IDX0102&file=IDX0102.201201250000.gif [Accessed 10 May 2016].

Bom.gov.au. (2016). [online] Available at: http://www.bom.gov.au/jsp/ncc/cdio/cvg/av [Accessed 17 Nov. 2016].

Bastin, S., Drobinski, P., Dabas, A., Delville, P., Reitebuch, O. and Werner, C. (2005). Impact of the Rhône and Durance valleys on sea-breeze circulation in the Marseille area. *Atmospheric Research*, 74(1-4), pp.303-328.

Cenedese, A. & Moniti, P. 2003. Interaction between an inland urban heat island and a sea-breeze flow: A laboratory study. *Journal of Applied Meteorology,* 42**,** 1569-1583.

Childs, P. and Raman, S. (2005). Observations and Numerical Simulations of Urban Heat Island and Sea Breeze Circulations over New York City. *Pure and Applied Geophysics*, 162(10), pp.1955-1980.

Clappier, A., Martilli, A., Grossi, P., Thunis, P., Pasi, F., Krueger, B., Calpini, B., Graziani, G. and van den Bergh, H. (2000). Effect of Sea Breeze on Air Pollution in the Greater Athens Area. Part I: Numerical Simulations and Field Observations. *Journal of Applied Meteorology*, 39(4), pp.546-562.

Crosman, E. and Horel, J. (2010). Sea and Lake Breezes: A Review of Numerical Studies. *Boundary-Layer Meteorology*, 137(1), pp.1-29.

Ding, A., Wang, T., Zhao, M., Wang, T. and Li, Z. (2004). Simulation of sea-land breezes and a discussion of their implications on the transport of air pollution during a multi-day ozone episode in the Pearl River Delta of China. *Atmospheric Environment*, 38(39), pp.6737-6750.

Frizzola, J. and Fisher, E. (1963). A Series of Sea Breeze Observations in the New York City Area. *Journal of Applied Meteorology*, 2(6), pp.722-739.

Emmanuel, R. and Johansson, E. (2006). Influence of urban morphology and sea breeze on hot humid microclimate: the case of Colombo, Sri Lanka. *Climate Research*, 30, pp.189-200.

Foken, T. and Nappo, C 2008, Micrometeorology, Berlin, Springer, p. 41.

Freitas, E., Rozoff, C., Cotton, W. and Dias, P. (2006). Interactions of an urban heat island and sea-breeze circulations during winter over the metropolitan area of São Paulo, Brazil. *Boundary-Layer Meteorology*, 122(1), pp.43-65.

Gedzelman, S., Austin, S., Cermak, R., Stefano, N., Partridge, S., Quesenberry, S. & Robinson, D. 2003. Mesoscale aspects of the urban heat island around New York City. *Theoretical and Applied Climatology,* 75**,** 29-42.

Gharib, S., and H. Guan (2015), Sea breeze cooling power in the Adelaide metropolitan area, in Australian Meteorological & Oceanographic Society National Conference 2015, Australian Meteorological & Oceanographic Society, Bresbane.

Gille, S., Lyewellyn Smith, S. and Statom, N. (2005). Global observations of the land breeze. *Geophysical Research Letters*, 32(5).

Guan, H., Soebarto, V., Bennett, J., Clay, R., Andrew, R., Guo, Y., Gharib, S. and Bellette, K. (2014). Response of office building electricity consumption to urban weather in Adelaide, South

Australia. *Urban Climate*, 10, pp.42-55.

Guan, H., Kumar, V., Clay, R., Kent, C., Bennett, J., Ewenz, C., Hopkins, G. and Simmons, C. (2016). Temporal and spatial patterns of air temperature in a coastal city with a slope base setting. Journal of Geophysical Research: Atmospheres, 121(10), pp.5336-5355.

Guan, H., Bennett, J., Ewenz, C., Benger, S., Kumar, V. and Zhu, S. (2013). *Characterisation, Interpretation and Implications of the Adelaide Urban Heat Island*. [online] Adelaide: The Flinders University, pp.10-16. Available at: http://dspace.flinders.edu.au/xmlui/handle/2328/26839 [Accessed 15 Jul. 2016].

Guan, H., Zhang, X., Makhnin, O , Sun, Z. 2013. Mapping mean monthly temperatures over a coastal hilly area incorporating terrain aspect effects. *Journal of Hydrometeorology,* 14**,** 233-250.

Hadi, T., Horinouchi, T., Tsuda, T., Hashiguchi, H. and Fukao, S. (2002). Sea-Breeze Circulation over Jakarta, Indonesia: A Climatology Based on Boundary Layer Radar Observations. *Monthly Weather Review*, 130(9), pp.2153-2166.

Hu, X. and Xue, M. (2016). Influence of Synoptic Sea-Breeze Fronts on the Urban Heat Island Intensity in Dallas–Fort Worth, Texas. *Mon. Wea. Rev.*, 144(4), pp.1487-1507.

Johnson, A. and O'brien, J. (1973). A Study of an Oregon Sea Breeze Event. *Journal of Applied Meteorology*, 12(8), pp.1267-1283.

Kagia, K. and Ashie, Y. National Research Project on Kaze-no-michi for City Planning: Creation of Ventilation Paths of Cool Sea Breeze in Tokyo. The Second International Conference (SICCUHI) on Co, 2009.

Kato, S. and Hiyama, K. (n.d.). *Ventilating cities*. 1st ed.

Kent, CA 2010, Characterising the Urban Heat Island of Adelaide during winter. Honours thesis, The Flinders University of South Australia.

Kumar, V., Guan, H., Bennett, C., Ewenz, C., Clay, R., Simmons, C.T., 2012, Influence of Parks on Urban Environment: A Real Case Numerical Study using WRF Mesoscale Model, International Conference on Urban Climate, Dublin.

Kusuda, M. and Alpert, P. (1983). Anti-Clockwise Rotation of the Wind Hodograph. Part I: Theoretical Study. J. Atmos. Sci., 40(2), pp.487-499.

Lalas, D., Asimakopoulos, D., Deligiorgi, D. and Helmis, C. (1983). Sea-breeze circulation and photochemical pollution in Athens, Greece. *Atmospheric Environment (1967)*, 17(9), pp.1621-1632.

Lin, C., Chen, F., Huang, J., Chen, W., Liou, Y., Chen, W. and Liu, S. (2008). Urban heat island effect and its impact on boundary layer development and land–sea circulation over northern Taiwan. *Atmospheric Environment*, 42(22), pp.5635-5649.

Lopes, A., Lopes, S., Matzarakis, A. and Alcoforado, M. (2011). The influence of the summer sea breeze on thermal comfort in Funchal (Madeira). A contribution to tourism and urban planning. *Meteorologische Zeitschrift*, 20(5), pp.553-564.

Loughner, C., Tzortziou, M., Follette-Cook, M., Pickering, K., Goldberg, D., Satam, C., Weinheimer, A., Crawford, J., Knapp, D., Montzka, D., Diskin, G. and Dickerson, R. (2014). Impact of Bay-Breeze Circulations on Surface Air Quality and Boundary Layer Export. *Journal of Applied Meteorology and Climatology*, 53(7), pp.1697-1713.

Lu, R. and Turco, R. (1994). Air Pollutant Transport in a Coastal Environment. Part I: Two-Dimensional Simulations of Sea-Breeze and Mountain Effects. *Journal of the Atmospheric Sciences*, 51(15), pp.2285-2308.

Lyons, T. (1975). Mesoscale wind spectra. *Quarterly Journal of the Royal Meteorological Society*, 101(430), pp.901-910.

Masuda, Y., Ikeda, N., Seno, T., Takahashi, N. and Ojima, T. (2005). A Basic Study on Utilization of the Cooling Effect of Sea Breeze in Waterfront Areas along Tokyo Bay. *Journal of Asian Architecture and Building Engineering*, 4(2), pp.483-487.

Mavrakou, T., Philippopoulos, K. and Deligiorgi, D. (2012). The impact of sea breeze under different synoptic patterns on air pollution within Athens basin. *Science of The Total Environment*, 433, pp.31-43.

Miao, J., Kroon, L., Vil-Guerau de Arellano, J. and Holtslag, A. (2003). Impacts of topography and land degradation on the sea breeze over eastern Spain. *Meteorology and Atmospheric Physics*, 84(3-4), pp.157-170.

Miller, S., Keim, B., Talbot, R. and Mao, H. 2003. Sea breeze: Structure, forecasting, and impacts. *Reviews of geophysics,* 41.

Muppa, S., Anandan, V., Kesarkar, K., Rao, S. and Reddy, P. (2012). Study on deep inland penetration of sea breeze over complex terrain in the tropics. *Atmospheric Research*, 104-105, pp.209-216.

Oke, T. (2006). *Instruments and Observing Methods*. World Meteorological Organization, p.11.

Papanastasiou, D., Melas, D., Bartzanas, T. and Kittas, C. (2009). Temperature, comfort and

pollution levels during heat waves and the role of sea breeze. *International Journal of Biometeorology*, 54(3), pp.307-317.

Pazandeh Masouleh, Z. (2015). *Identification of Sea Breeze, their Climate Trends and Causation, with Application to the Adelaide Coast*. Ph.D. The University of Adelaide.

Physick, W. & Byron-Scott, R. 1977. Observations of the sea breeze in the vicinity of a gulf. *Weather,* 32**,** 373-381.

Physick, W. (1976). A Numerical Model of the Sea-Breeze Phenomenon over a Lake or Gulf. J. Atmos. Sci., 33(11), pp.2107-2135.

Pielke, R. (1974). A Three-Dimensional Numerical Model of the Sea Breezes Over South Florida. *Monthly Weather Review*, 102(2), pp.115-139.

Robinson, F., Patterson, M. and Sherwood, S. (2013). A Numerical Modeling Study of the Propagation of Idealized Sea-Breeze Density Currents*. *Journal of the Atmospheric Sciences*, 70(2), pp.653-668.

Sashiyama, S. & Yamamoto, K. 2014. Method for Evaluating the Influence of Obstruction of Sea Breeze by Clusters of High-Rise Buildings on the Urban Heat Island Effect. *Journal of Environmental Protection,* 5**,** 983.

Steele, C., Dorling, S., von Glasow, R. and Bacon, J. (2014). Modelling sea-breeze climatologies and interactions on coasts in the southern North Sea: implications for offshore wind energy. *Quarterly Journal of the Royal Meteorological Society*, 141(690), pp.1821-1835.

Sturman, A. P., Tapper, N. J.1996. *The weather and climate of Australia and New Zealand*, Oxford University Press Melbourne.

Simpson, J. (1994). *Sea breeze and local winds*. 1st ed. Cambridge: Cambridge University Press, pp.1-27.

Simpson, J. (1967). AERIAL AND RADAR OBSERVATIONS OF SOME SEA-BREEZE FRONTS. *Weather*, 22(8), pp.306-316.

Suresh, R. (2007). Observation of Sea Breeze Front and its Induced Convection over Chennai in Southern Peninsular India Using Doppler Weather Radar. *Pure and Applied Geophysics*, 164(8-9), pp.1511-1525.

Wakimoto, R. and Atkins, N. (1994). Observations of the Sea-Breeze Front during CaPE. Part I: Single-Doppler, Satellite, and Cloud Photogrammetry Analysis. *Monthly Weather Review*, 122(6), pp.1092-1114.